



Two New Species of *Diploderma* Hallowell, 1861 (Reptilia: Squamata: Agamidae) from the Hengduan Mountain Region in China and Rediscovery of *D. brevicaudum* (Manthey, Wolfgang, Hou, Wang, 2012)

KAI WANG^{1,2,6*}, WEI GAO^{1,4,7}, JIAWEI WU³, WENJIE DONG^{1,4,8}, XIAOGANG FENG^{1,4,9},
WENJING SHEN^{1,10}, JIEQIONG JIN^{1,11}, XIUDONG SHI^{5,12}, YIN QI^{5,13},
CAMERON D. SILER^{2,14} & JING CHE^{1,15*}

¹State Key Laboratory of Genetic Resources and Evolution, Kunming Institute of Zoology, Chinese Academy of Sciences, Kunming, Yunnan 650223, China

²Sam Noble Oklahoma Museum of Natural History and Department of Biology, University of Oklahoma, Norman, Oklahoma 73072-7029, USA

³Swild Studio, Chengdu, Sichuan 610015, China.

✉ wujiawei@swild.cn; <https://orcid.org/0000-0002-7668-7748>

⁴Kunming College of Life Science, University of the Chinese Academy of Sciences, Kunming, Yunnan, 650204, China

⁵Chengdu Institute of Biology, Chinese Academy of Sciences, Chengdu, Sichuan 610041, China

✉ kai.wang-2@ou.edu; <https://orcid.org/0000-0002-6736-3346>

✉ gaowei1160@163.com; <https://orcid.org/0000-0002-4539-1186>

✉ dwjddaniel@foxmail.com; <https://orcid.org/0000-0002-3201-4533>

✉ fengxiaogang@mail.kiz.ac.cn; <https://orcid.org/0000-0002-2145-9078>

¹⁰✉ shenwenjing@mail.kiz.ac.cn; <https://orcid.org/0000-0003-2144-1844>

¹¹✉ jinqj@mail.kiz.ac.cn; <https://orcid.org/0000-0003-1603-9914>

¹²✉ shixd@cib.ac.cn; <https://orcid.org/0000-0002-0860-8622>

¹³✉ qiyin@cib.ac.cn; <https://orcid.org/0000-0003-0973-2307>

¹⁴✉ camsiler@ou.edu; <https://orcid.org/0000-0002-7573-096X>

¹⁵✉ chej@kiz.ac.cn; <https://orcid.org/0000-0003-4246-6514>

*Corresponding authors

Abstract

Recent studies have highlighted the underestimated diversity of the genus *Diploderma* Hallowell, 1861 in the Hengduan Mountain Region in Southwest China, but much of the region remains poorly surveyed for reptile diversity. In this study we describe two new species of *Diploderma* from the upper Jinsha and middle Yalong River Valley, based on evaluations of morphological, genetic, and distribution data. The two new species are morphologically most similar to *D. angustelinea* and *D. vela*, but they can be diagnosed from both recognized taxa and all remaining congeners by a suite of morphological features, particularly the distinct coloration of gular spots. Additionally, both new species either render other recognized species paraphyletic or are allopatric with respect to their morphologically similar congeners. Furthermore, we rediscover *D. brevicaudum* in the wild for the first time, which was known from historical museum specimens only. We estimate the phylogenetic position of *D. brevicaudum* within the genus *Diploderma* based on mitochondrial genealogy, and we provide an expanded diagnosis and comparisons against closely related congeners and provide a detailed description of coloration in life based on newly collected specimens. Our discoveries of the new *Diploderma* species further highlight the urgent conservation needs of the currently neglected hot-dry valley ecosystems in the Hengduan Mountain Region of China.

Key words: conservation, cryptic diversity, hot-dry valley, micro-endemism, ornamentation, Yangtze

Introduction

Mountain Dragons of the genus *Diploderma* Hallowell, 1861 represent a unique agamid radiation in East Asia, including 32 species currently recognized (Wang *et al.* 2019a, 2019b, 2019c, 2020b; Liu *et al.* 2020). Of the total diversity, 21 species are only distributed in the Hengduan Mountain Region (HMR) of Southwest China, and 13 of

the 21 HMR species were described recently from the *D. flaviceps* (Barbour, Dunn, 1919) complex in the past eight years (Manthey *et al.* 2012; Wang *et al.* 2016, 2019d, e, 2020a, 2020b). Despite the continuous discoveries of new taxa, the most recent taxonomic study still suggests the presence of additional, unrecognized diversity within the *D. flaviceps* complex in the HMR, particularly populations of previously identified *D. cf. flaviceps* along the upper Jinsha and Yalong Rivers (Wang *et al.* 2020b).

Relating to the issue of cryptic diversity, species boundaries and basic biological data of many recognized species within the genus remain unknown, which hinders the clarification of the taxonomy, the discovery of new taxa, and the protection of micro-endemic lineages. To date, three recognized species, namely *D. brevicaudum* (Manthey, Wolfgang, Hou, Wang, 2012), *D. grahami* (Stejneger, 1924), and *D. hamptoni* (Smith, 1935), are still known only from the type specimens, all collected more than a century ago (Wang *et al.* 2017; Denzer *et al.* 2019). Among the three species, *D. brevicaudum* is the only one that has multiple type specimens (holotype: AMNH 19879; paratypes: AMNH 19878, NMW 20853, and ZMB 28932; see method section for museum acronyms) and a more detailed original description (Manthey *et al.* 2012). However, despite the recent description of *D. brevicaudum*, it is still known from these four historical type specimens only, and no additional information is available regarding its coloration in life, natural history, or phylogenetic relationship within the genus *Diploderma*.

During herpetological surveys of the HMR in 2019, specimens of the genus *Diploderma* were collected from the upper Jinsha River Valley in Northwest Yunnan Province and middle Yalong River Valley in southern Sichuan Province, China. Subsequent morphological comparison confirmed that the specimens from the type locality of *D. brevicaudum* in Lijiang, Yunnan Province match the original description of the species (Manthey *et al.* 2012). In contrast, specimens collected from the upper Jinsha River in Deqin County and from the middle Yalong River in Muli County were identifiable as members of the *D. flaviceps* complex, but they could not be assigned to any recognized species. Herein, we conducted phylogenetic and morphological analyses that indicate the Deqin and Muli populations represent two distinct, undescribed lineages. We describe the Deqin and Muli populations as two new species of the *Diploderma flaviceps* complex. Additionally, we expand the diagnosis of *D. brevicaudum* and provide the first description of coloration in life based on the newly collected specimens, estimate its phylogenetic placement within the genus, and provide an assessment of its conservation status based on our survey data.

Materials and methods

Sampling

A total of four specimens of the putative new species 1 were collected in the Yalong River Valley near Bowo Village, Muli County, Sichuan Province, China on 25 June 2019 (Fig. 1, star 1), and eight specimens of the putative new species 2 (Fig. 1, star 2) were collected along the upper Jinsha Valley near Yangla Village, Deqin County, Yunnan Province, China on 17 June 2019. Additionally, four specimens of *D. cf. brevicaudum* were collected from areas near Lijiang City on 4 June 2019 (Fig. 1, circle 17), and another female was collected from Shangjiang Village in Shangrila County, Yunnan Province, China on 10 July 2016 (Fig. 1, triangle). After euthanasia, genetic samples (liver or muscle) were taken and stored in 95% ethanol, while the specimens were vouchered in 10% buffered formalin and transferred to 75% ethanol after fieldwork. All specimens were deposited at the Museum of Kunming Institute of Zoology, Chinese Academy of Sciences (KIZ).

In addition to the newly collected specimens, we also examined 282 specimens of 28 recognized congeners from the following natural history museum collections: Chengdu Institute of Biology, Chinese Academy of Sciences, China (CIB); Natural History Museum, UK (BMNH); California Academy of Sciences, USA (CAS); KIZ; National Museum of Natural History, USA (USNM); and Museum of Comparative Zoology, USA (MCZ) (Appendix I). Furthermore, the following acronyms of museums were used: American Museum of Natural History (AMNH), Naturhistorisches Museum, Wien (NMW), and Museum für Naturkunde, Leibniz-Institut für Evolutions- ZMB und Biodiversitätsforschung an der Humboldt-Universität (ZMB).

Morphological data

Specimens were measured using a digital caliper to the nearest 0.1 mm, except for tail length, which was measured to the nearest 1 mm using a ruler. The following morphometric characters were measured following Wang *et al.* (2020b) (abbreviations given in parentheses): snout–vent length (SVL), tail length (TAL), head length (HL),

head width (HW), head depth (HD), snout–eye length (SEL), fore-limb length (FLL), hind limb length (HLL), Toe IV length (T4L; excluding the claw), and trunk length (TRL). In addition, the following pholidosis characters were recorded: supralabial scale count (SL), infralabial scale count (IL), middorsal scale count (MD), Finger IV subdigital lamellae count (F4S), Toe IV subdigital lamellae count (T4S), number of scales between nasal and first supralabials (NSL), number of scale rows between supralabials and orbit circle (SOR), enlarged, modified, post-occipital scale count (POS), enlarged, modified, post-tympanic scale count (PTY), and enlarged, modified, post-ribral scale count (PRS). Measurements were taken on the left side of the specimen only (unless the left side was damaged, then the right side was used), and values for paired pholidosis characters (SL, IL, NSL, SCL, SOR, PTY, and PRS) were recorded on both sides of the body, with counts provided in left/right order.

The following coloration and ornamentation patterns were examined following Wang *et al.* (2020b): coloration of the oral cavity (CO), defined as the background coloration of the anterior roof and sides of the mouth, excluding the posterior palate and deep throat; coloration of the tonsil (CT), defined as the coloration of the posterior palate and tonsil; coloration of the tongue (CTG), defined as the coloration of the tongue; coloration of dorsolateral stripes (CDS), defined as the background coloration of the dorsolateral stripes; and the shape of dorsolateral stripes (SDS), defined as the shape of dorsolateral stripe in males, either smooth edged or jagged. Color names and codes for coloration followed Köhler (2012).

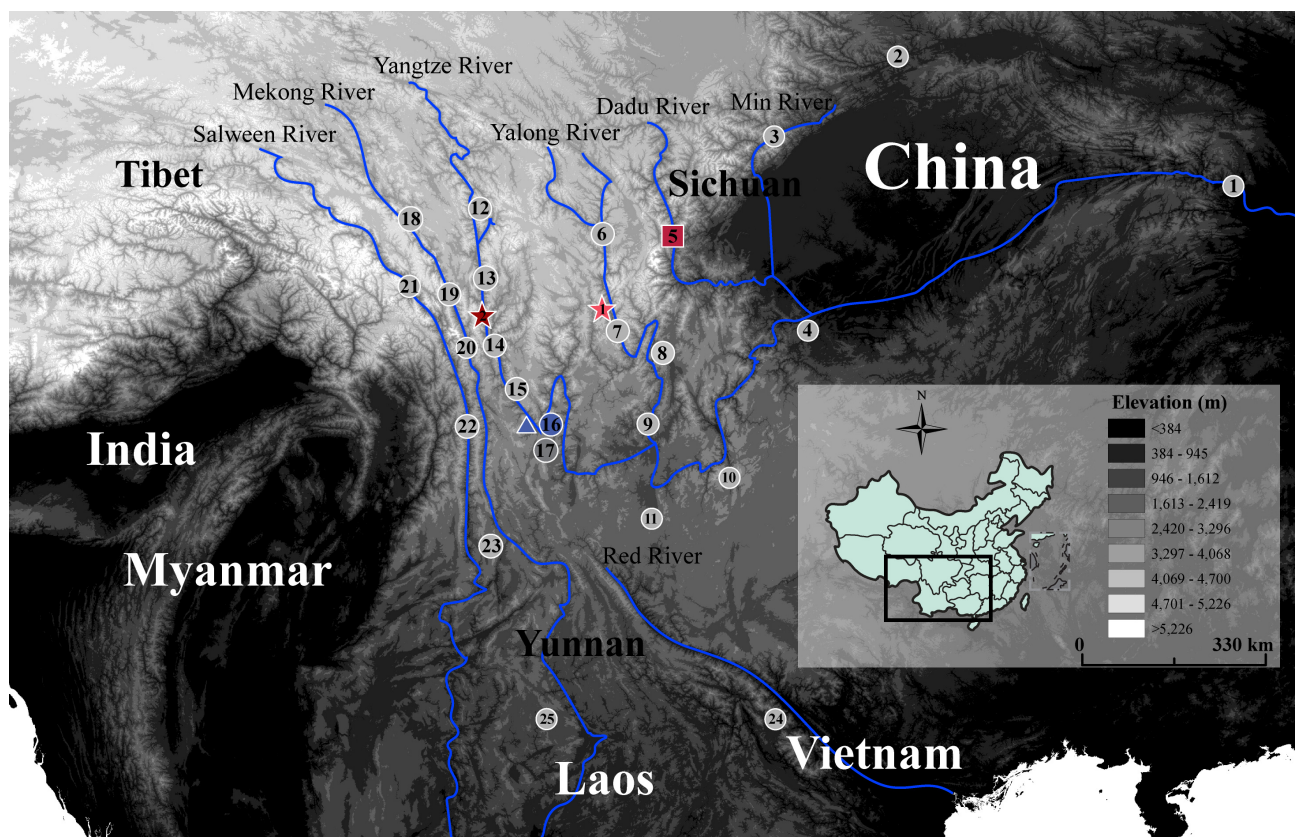


FIGURE 1. Distributions of *Diploderma* species in Southwest China. Numbered shapes represent type localities of *Diploderma* species: the rectangle represents true *D. flaviceps* (5), stars represent the two new species described in this study (1: *D. bowoense* sp. nov.; 2: *D. formosgulae* sp. nov.), and circles represent type localities of the remaining recognized congeners (1: *D. splendidum*; 2: *D. micangshanense*; 3: *D. zhaoermii*; 4: *D. grahami*; 6: *D. panchi*; 7: *D. angustelinea*; 8: *D. panlong*; 9: *D. swild*; 10: *D. dymondi*; 11: *D. varcoae*; 12: *D. flavilabre*; 13: *D. batangense*; 14: *D. aorun*; 15: *D. qilin*; 16: *D. brevicaudum*; 17: *D. yulongense*; 18: *D. drukdaypo*; 19: *D. vela*; 20: *D. iadinum*; 21: *D. laeiventre*; 22: *D. slowinskii*; 23: *D. yunnanense*; 24: *D. chapaense*; and 25: *D. menghaiense*). The white triangle represents a new locality of *D. brevicaudum* in Shangjiang Village, Shangri-La County, Yunnan, China.

Molecular Data

Total genomic DNA was extracted for the two putative new species and *D. cf. brevicaudum* from liver or muscle tissues with a standard three-step phenol-chloroform extraction method (Sambrook *et al.* 1982). The mitochondrial gene NADH dehydrogenase subunit 2 (*ND2*, 1035bp [coding region], 182bp [tRNAs]) was targeted and amplified using published primers (Jap_70F, Jap_1559R; Wang *et al.* 2019a). PCR and sequencing methods followed recent published protocols (Wang *et al.* 2020b).

Phylogenetic Analyses

In addition to the newly generated sequences, matching *ND2* data for 26 species of *Diploderma* and representatives of *Calotes*, *Pseudocalotes*, and *Acanthosaura* were obtained from GenBank (Appendix II). Outgroup taxa were chosen based on the recent phylogenetic study of the subfamily Draconinae (Wang *et al.* 2019a). All sequences were edited and aligned using MUSCLE in Geneious v. 10.0.6. The final alignment contained 1031bp, with 10 novel sequences deposited in GenBank (Table 1).

Bayesian inference (BI) and Maximum Likelihood (ML) analyses were conducted on the final alignment. Bayesian analysis was done using the program MrBayes v. 3.2.6 (Ronquist *et al.* 2012). The *ND2* coding region was partitioned by codon position, and entire fragment (182bp total) of tRNAs was treated as a single partition. Using JMODELTEST2 v. 2.1.10 (Guindon & Gascuel 2003; Darriba *et al.* 2012), the best evolutionary model of nucleotide substitution was selected for each partition, which inferred the model GTR + Γ for all partitions. Two independent Markov Chain Monte Carlo analyses were run, each with four Metropolis-coupled chains, a melting temperature of 0.02, and an exponential distribution with a rate parameter of 25 as the prior on branch lengths (Marshall 2010). Each run was conducted with 90 million generations and sampled every 2,000 generations, discarding the first 20% of trees as burnin. Finally, we confirmed convergence of runs with TRACER v. 1.6.0 (visual convergence and ESS>200; Rambaut *et al.* 2013).

Maximum Likelihood analysis was conducted using RAxML-VI-HPC v. 8.2.10 (Stamatakis, 2014). The most complex model (GTR + Γ) was applied to all partitions, with 1,000 replicate ML inference runs. We initiated each inference with a random starting tree and assessed nodal support with 1,000 bootstrap pseudoreplicates (Stamatakis *et al.* 2008). Finally, uncorrected genetic pairwise distances (p-distances) were obtained for the coding region of *ND2* (1035bp) using PAUP v. 4.0b10 (Swofford 2003).

TABLE 1. GenBank accession numbers for the samples used in the present study. New sequences are indicated in bold. “–” indicates locality information not available.

Vouchered Number	Species	Locality	GenBank Accession Number
KIZ 044757	<i>Diploderma bowoense</i> sp. nov.	Muli, Sichuan, China	MW506020
KIZ 044758	<i>D. bowoense</i> sp. nov.	Muli, Sichuan, China	MW506019
KIZ 044420	<i>D. formosgulae</i> sp. nov.	Deqin, Yunnan, China	MW506024
KIZ 044421	<i>D. formosgulae</i> sp. nov.	Deqin, Yunnan, China	MW506025
KIZ 044373	<i>D. formosgulae</i> sp. nov.	Deqin, Yunnan, China	MW506028
KIZ 044375	<i>D. formosgulae</i> sp. nov.	Deqin, Yunnan, China	MW506026
KIZ 044376	<i>D. formosgulae</i> sp. nov.	Deqin, Yunnan, China	MW506027
KIZ 044304	<i>D. brevicaudum</i>	Lijiang, Yunnan, China	MW506023
KIZ 044305	<i>D. brevicaudum</i>	Lijiang, Yunnan, China	MW506021
KIZ 044306	<i>D. brevicaudum</i>	Lijiang, Yunnan, China	MW506022
KIZ 029704	<i>D. angustelinea</i>	Muli, Sichuan, China	MT577930
KIZ 029705	<i>D. angustelinea</i>	Muli, Sichuan, China	MT577924
KIZ 029708	<i>D. angustelinea</i>	Muli, Sichuan, China	MT577931
KIZ 029710	<i>D. angustelinea</i>	Muli, Sichuan, China	MT577927
KIZ 032488	<i>D. angustelinea</i>	Muli, Sichuan, China	MT577925
KIZ 032489	<i>D. angustelinea</i>	Muli, Sichuan, China	MT577926

.....continued on the next page

TABLE 1. (Continued)

Vouchered Number	Species	Locality	GenBank Accession Number
KIZ 032490	<i>D. angustelinea</i>	Muli, Sichuan, China	MT577928
KIZ 032491	<i>D. angustelinea</i>	Muli, Sichuan, China	MT577929
KIZ 032733	<i>D. aorun</i>	Benzilan, Yunnan, China	MT577938
KIZ 032734	<i>D. aorun</i>	Benzilan, Yunnan, China	MT577939
KIZ 032735	<i>D. aorun</i>	Benzilan, Yunnan, China	MT577937
KIZ 032736	<i>D. aorun</i>	Benzilan, Yunnan, China	MT577936
KIZ 032737	<i>D. aorun</i>	Benzilan, Yunnan, China	MT577940
KIZ 019278	<i>D. batangense</i>	Zhubalong, Markam, Tibet, China	MT577932
KIZ 019279	<i>D. batangense</i>	Zhubalong, Markam, Tibet, China	MT577933
KIZ 019276	<i>D. batangense</i>	Batang, Sichuan, China	MK001413
KIZ 09404	<i>D. batangense</i>	Zhubalong, Tibet, China	MK001412
KIZ 019281	<i>D. batangense</i>	Batang, Sichuan, China	MT577934
KIZ 019314	<i>D. batangense</i>	Zhubalong, Markam, Tibet, China	MT577935
NMNS 19607	<i>D. brevipes</i>	Taiwan, China	MK001429
NMNS 19608	<i>D. brevipes</i>	Taiwan, China	MK001430
KIZ 034923	<i>D. chapaense</i>	Lvchun, Honghe, Yunnan, China	MG214263
KIZ 040145	<i>D. chapaense</i>	Dali, Yunnan, China	MK578667
KIZ 046954	<i>D. chapaense</i>	Jingdong, Yunnan, China	MK578660
KIZ 046970	<i>D. chapaense</i>	Jingdong, Yunnan, China	MK578659
KIZ 047085	<i>D. chapaense</i>	Jingdong, Yunnan, China	MK578661
KIZ 034921	<i>D. chapaense</i>	Lvchun, Yunnan, China	MG214264
ZMMU NAP-01911	<i>D. chapaense</i>	Chapa, Vietnam	MG214262
KIZ 027627	<i>D. drukdaypo</i>	Jinduo, Chamdo, Tibet, China	MT577950
KIZ 027628	<i>D. drukdaypo</i>	Zhuka, Chamdo, Tibet, China	MT577592
KIZ 027629	<i>D. drukdaypo</i>	Zhuka, Chamdo, Tibet, China	MT577593
KIZ 016486	<i>D. drukdaypo</i>	Chamdo City, Tibet, China	MT577951
KIZ 027630	<i>D. drukdaypo</i>	Zhuka, Chamdo, Tibet, China	MT577954
KIZ 040147	<i>D. dymondi</i>	Panzhuhua, Sichuan, China	MT577899
KIZ 040148	<i>D. dymondi</i>	Panzhuhua, Sichuan, China	MT577900
KIZ 040149	<i>D. dymondi</i>	Panzhuhua, Sichuan, China	MT577901
KIZ 040639	<i>D. dymondi</i>	Dongchuan, Yunnan, China	MK001422
KIZ 040640	<i>D. dymondi</i>	Dongchuan, Yunnan, China	MK001423
KIZ 019575	<i>D. flaviceps</i>	Kangding, Sichuan, China	MT577896
KIZ 019576	<i>D. flaviceps</i>	Kangding, Sichuan, China	MT577897
KIZ 019577	<i>D. flaviceps</i>	Kangding, Sichuan, China	MT577895
KIZ 019578	<i>D. flaviceps</i>	Kangding, Sichuan, China	MT577894
KIZ 019579	<i>D. flaviceps</i>	Kangding, Sichuan, China	MT577898
KIZ 01851	<i>D. flaviceps</i>	Luding, Sichuan, China	MK001416
KIZ 01852	<i>D. flaviceps</i>	Luding, Sichuan, China	MK001417
KIZ 032692	<i>D. flavilabre</i>	Baiyu, Sichuan, China	MT577916
KIZ 032694	<i>D. flavilabre</i>	Baiyu, Sichuan, China	MT577917
KIZ 032695	<i>D. flavilabre</i>	Baiyu, Sichuan, China	MT577918

.....continued on the next page

TABLE 1. (Continued)

Vouchered Number	Species	Locality	GenBank Accession Number
KIZ 032696	<i>D. flavilabre</i>	Baiyu, Sichuan, China	MT577919
KIZ 032697	<i>D. flavilabre</i>	Baiyu, Sichuan, China	MT577915
KIZ 032698	<i>D. flavilabre</i>	Baiyu, Sichuan, China	MT577920
KIZ 027697	<i>D. iadinum</i>	Degong Village, Yunling, Deqin, Yunnan, China	MT577956
KIZ 027702	<i>D. iadinum</i>	Degong Village, Yunling, Deqin, Yunnan, China	MT577957
KIZ 027706	<i>D. iadinum</i>	Degong Village, Yunling, Deqin, Yunnan, China	MT577955
KIZ 027691	<i>D. laeviventre</i>	Basu, Markam, Tibet, China	MT577892
KIZ 027692	<i>D. laeviventre</i>	Basu, Markam, Tibet, China	MT577893
KIZ 014037	<i>D. laeviventre</i>	Basu, Markam, Tibet, China	MK001407
NMNS 19604	<i>D. luei</i>	Taiwan, China	MK001433
NMNS 19605	<i>D. luei</i>	Taiwan, China	MK001434
NMNS 19609	<i>D. makii</i>	Taiwan, China	MK001431
NMNS 19610	<i>D. makii</i>	Taiwan, China	MK001432
KIZ 023231	<i>D. micangshanense</i>	Xixia, Henan, China	MK578664
KIZ 032801	<i>D. micangshanense</i>	Shiyan, Hubei, China	MK578665
KIZ 032802	<i>D. micangshanense</i>	Shiyan, Hubei, China	MK578666
KIZ 06850	<i>D. micangshanense</i>	Longnan, Gansu, China	MK001424
WK-JK 037	<i>D. micangshanense</i>	Wenxian, Gansu, China	MK578662
WK-JK 038	<i>D. micangshanense</i>	Wenxian, Gansu, China	MK578663
KIZ 032715	<i>D. panchi</i>	Yajiang, Sichuan, China	MT577946
KIZ 032716	<i>D. panchi</i>	Yajiang, Sichuan, China	MT577944
KIZ 032717	<i>D. panchi</i>	Yajiang, Sichuan, China	MT577947
KIZ 032729	<i>D. panchi</i>	Yajiang, Sichuan, China	MT577945
KIZ 040137	<i>D. panlong</i>	Miansha, Liangshan, Sichuan, China	MT577906
KIZ 040138	<i>D. panlong</i>	Miansha, Liangshan, Sichuan, China	MT577907
KIZ 040139	<i>D. panlong</i>	Miansha, Liangshan, Sichuan, China	MT577908
KIZ 040140	<i>D. panlong</i>	Miansha, Liangshan, Sichuan, China	MT577905
KIZ 040141	<i>D. panlong</i>	Miansha, Liangshan, Sichuan, China	MT577909
KIZ 040143	<i>D. panlong</i>	Miansha, Liangshan, Sichuan, China	MT577904
NMNS 19598	<i>D. polygonatum</i>	Taiwan, China	MK001427
NMNS 19599	<i>D. polygonatum</i>	Taiwan, China	MK001428
KIZ 028332	<i>D. qilin</i>	Balong, Deqin, Yunnan, China	MT577941
KIZ 028335	<i>D. qilin</i>	Balong, Deqin, Yunnan, China	MT577943
KIZ 028333	<i>D. qilin</i>	Balong, Deqin, Yunnan, China	MT577942
KIZ 027543	<i>D. slowinskii</i>	Fugong, Gongshan, Yunnan, China	MT577910
KIZ 027544	<i>D. slowinskii</i>	Fugong, Gongshan, Yunnan, China	MT577911
KIZ 027572	<i>D. slowinskii</i>	Qiunatong, Gongshan, Yunnan, China	MT577912
KIZ 027573	<i>D. slowinskii</i>	Qiunatong, Gongshan, Yunnan, China	MT577913
CAS 214906	<i>D. slowinskii</i>	Gongshan, Yunnan, China	MK001405
CAS 214954	<i>D. slowinskii</i>	Gongshan, Yunnan, China	MK001406

.....continued on the next page

TABLE 1. (Continued)

Vouchered Number	Species	Locality	GenBank Accession Number
KIZ 015973	<i>D. splendidum</i>	Yichang, Hubei, China	MK001418
CAS 194476	<i>D. splendidum</i>	Yaan, Sichuan, China	AF128501
KIZ 034893	<i>D. swild</i>	Panzhuhua, Sichuan, China	MN266297
KIZ 034894	<i>D. swild</i>	Panzhuhua, Sichuan, China	MN266300
KIZ 034895	<i>D. swild</i>	Panzhuhua, Sichuan, China	MN266298
KIZ 034914	<i>D. swild</i>	Panzhuhua, Sichuan, China	MN266299
KIZ 034915	<i>D. swild</i>	Panzhuhua, Sichuan, China	MN266301
NMNS 19592	<i>D. swinhonis</i>	Taiwan, China	MK001419
NMNS 19593	<i>D. swinhonis</i>	Taiwan, China	MK001420
KIZ 029711	<i>D. varcoae</i>	Dali, Yunnan, China	MT577902
WK-JK 011	<i>D. varcoae</i>	Yuxi, Yunnan, China	MT577903
KIZ 026132	<i>D. varcoae</i>	Mengzi, Honghe, Yunnan, China	MK001421
KIZ 027672	<i>D. vela</i>	Tongsha, Markam, Tibet, China	MT577949
KIZ 027673	<i>D. vela</i>	Tongsha, Markam, Tibet, China	MT577948
KIZ 034925	<i>D. vela</i>	Quzika, Markam, Tibet, China	MK001415
KIZ 019299	<i>D. vela</i>	Quzika, Markam, Tibet, China	MK001414
KIZ 028291	<i>D. yulongense</i>	Middle Hutiaoxia, Shangrila, Yunnan, China	MT577921
KIZ 028292	<i>D. yulongense</i>	Middle Hutiaoxia, Shangrila, Yunnan, China	MT577922
KIZ 028300	<i>D. yulongense</i>	Baishuitai, Shangrila, Yunnan, China	MT577923
KIZ 09399	<i>D. yulongense</i>	Xianggelila, Yunnan, China	MK001410
KIZ 43196	<i>D. yulongense</i>	Xianggelila, Yunnan, China	MK001411
KIZ 040193	<i>D. yunnanense</i>	Yingjiang, Yunnan, China	MT577914
KIZ 040193	<i>D. yunnanense</i>	Yingjiang, Yunnan, China	MK578658
CAS 242271	<i>D. yunnanense</i>	Baoshan, Yunnan, China	MK001408
CAS 242183	<i>D. yunnanense</i>	Baoshan, Yunnan, China	MK001409
KIZ 019564	<i>D. zhaoermii</i>	Wenchuan, Sichuan, China	MK001425
KIZ 019565	<i>D. zhaoermii</i>	Wenchuan, Sichuan, China	MK001426
MVZ 216622	<i>D. zhaoermii</i>	Wenchuan, Sichuan, China	AF128500
–	<i>Acanthosaura lepidogaster</i>	–	AF128499
CAS 223063	<i>Calotes emma</i>	–	DQ289460
CIB 091468	<i>C. versicolor</i>	Hainan, China	KC875820
MVZ 224106	<i>Pseudocalotes brevipes</i>	Vinh Phuc, Vietnam	AF128499.1
TNHC 58040	<i>P. flavigula</i>	Perak, Malaysia	AF128503.1
CAS 241966	<i>P. kingdonwardi</i>	Dulongjiang, Yunnan, China	MK001436
CAS 242628	<i>P. kingdonwardi</i>	Dulongjiang, Yunnan, China	MK001437
KIZ 015975	<i>P. kakhensis</i>	Gongshan, Yunnan, China	MK001435

TABLE 2. Morphological data of the newly collected specimens of *Diploderma brevicaudum*. All morphometric measurements are in the unit of mm, and all paired pholidosis characters are recorded from both sides of the body and are given in left/right order. For measurement methods and abbreviations, see the Methods section. “–” indicates missing data due to an incomplete tail.

Voucher number	KIZ 044497	KIZ 044306	KIZ 028338	KIZ 044305
Sex	M	M	F	F
SVL	56.8	57.2	63.4	65.2
TAL	104.7	–	101.0	89.2
HL	18.0	17.8	18.1	18.1
HW	12.3	12.4	13.5	12.6
HD	8.6	9.1	10.1	9.3
SEL	6.9	7.3	6.6	7.1
FLL	27.7	24.7	27.5	26.8
HLL	45.9	40.8	44.4	43.7
T4L	11.7	10.0	10.7	10.5
TRL	23.8	26.2	33.2	31.2
TAL/SVL	184.1%	–	159.1%	136.8%
SEL/HL	38.1%	41.1%	36.4%	39.1%
HW/HL	68.5%	69.7%	74.8%	69.6%
HD/HW	70.2%	73.7%	74.4%	73.4%
FLL/SVL	48.7%	43.1%	43.4%	41.1%
HLL/SVL	80.8%	71.4%	70.0%	67.1%
TRL/SVL	41.9%	45.7%	52.3%	47.8%
SL	9/9	9/8	9/9	8/9
IL	9/9	10/10	10/9	11/10
NSL	2/2	1/2	1/1	1/1
MD	39	41	43	43
F4S	15/15	16/16	14/15	16/17
T4S	22/21	21/20	19/19	23/21
SOR	3/3	3/3	3/3	4/4
PTS	3/3	4/4	3/4	4/5
PTY	4/4	6/5	3/2	4/5
PRS	5/6	6/6	3/5	7/8

Results

Morphological Results

Newly collected specimens of *D. cf. brevicaudum* align closely with the type series of the species, except for two specimens that possess longer tails (TAL 184.1% SVL in male KIZ 044497, 159.1% in female KIZ 028338 vs. $\leq 150\%$ in original description), and the newly collected individuals possess longer fore-limbs (FLL 41.1–48.7% SVL vs. $\leq 39.5\%$ in original description) (Table 2). The morphological differences can be explained by the limited sample size of the type series as well as the potentially different methods of measurement for limb lengths by authors in the original description (Manthey *et al.* 2012).

Both putative new species, which were confused as *D. flaviceps*, can be differentiated from all recognized congeners by a suite of morphological characters, especially gular coloration and ornamentation in both sexes (Fig. 3). Putative new species 1 from Muli County is morphologically most similar and closest geographically to *D. angustelinea*, but it can be differentiated by having a shorter tail (vs. much longer), better developed nuchal and dorsal crest with skin folds in males (vs. feebly developed or absence), and by the presence of distinct dark vermiculate

TABLE 3. Uncorrected pairwise genetic distance of selected species of the genus *Diploderma* from the HMR based on the coding region of the mitochondrial *ND2* gene (1031 bp). Intraspecific genetic distances were indicated in bold.

	1	2	3	4	5	6	7
1	<i>D. bowoense</i> sp. nov.	0.3					
2	<i>D. formosugulae</i> sp. nov.	9.2–9.5	0–0.3				
3	<i>D. angustelinea</i>	8.7–9.3	6.6–7.3	0–0.1			
4	<i>D. aorun</i>	9.3–9.7	5.3–5.6	8.1–8.7	0–0.7		
5	<i>D. batangense</i>	8.7–9.1	6.6–7.6	7.5–8.4	8.0–8.6	0–0.4	
6	<i>D. brevicaudum</i>	8.8–8.9	4.4–4.7	6.8–7.0	5.2–5.5	6.3–7.1	0–0.1
7	<i>D. drukdaypo</i>	9.2–9.6	2.8–3.3	6.8–7.5	4.9–5.3	6.9–7.8	4.1–4.4
8	<i>D. flaviceps</i>	18.8–19.8	17.7–18.7	18.5–19.2	18.6–19.7	17.1–18.7	17.5–18.5
9	<i>D. panchi</i>	9.3–10.0	4.5–4.9	7.7–8.2	4.7–5.2	6.6–7.1	5.1–5.4
10	<i>D. panlong</i>	17.3–18.4	16.5–17.2	17.0–17.9	17.4–18.7	15.2–16.6	16.1–17.1
11	<i>D. qilin</i>	9.0–9.1	4.7–5.1	7.0–7.3	5.7–6.0	6.6–7.0	4.0–4.1
12	<i>D. swild</i>	17.4–18.1	15.9–16.7	16.8–17.3	17.6–18.5	15.2–16.2	16.1–17.0
13	<i>D. vela</i>	9.1–9.4	3.2–3.4	7.1–7.5	5.2–5.5	6.7–7.3	4.7–4.9
14	<i>D. yulongense</i>	9.5–9.7	6.9–7.4	7.7–8.3	8.1–8.5	8.0–8.8	6.8–7.1

TABLE 3. (Continued)

	8	9	10	11	12	13	14
1	<i>D. bowoense</i> sp. nov.						
2	<i>D. formosugulae</i> sp. nov.						
3	<i>D. angustelinea</i>						
4	<i>D. aorun</i>						
5	<i>D. batangense</i>						
6	<i>D. brevicaudum</i>						
7	<i>D. drukdaypo</i>						
8	<i>D. flaviceps</i>	0.1–1.5					
9	<i>D. panchi</i>	17.6–19.4	0–0.2				
10	<i>D. panlong</i>	15.3–16.1	16.0–17.6	0–2.8			
11	<i>D. qilin</i>	18.3–19.1	5.7–6.0	17.0–17.8	0–0.1		
12	<i>D. swild</i>	15.6–16.3	16.5–17.4	9.6–10.4	16.7–17.3	0–0.3	
13	<i>D. vela</i>	18.4–19.1	5.2–5.8	16.1–17.0	4.6–4.8	16.2–16.8	0–0.1
14	<i>D. yulongense</i>	18.7–19.6	8.6–8.9	17.2–18.2	7.6–7.8	17.6–18.4	7.9–8.2

stripes on the ventral surface of the head in both sexes (vs. absence) (details see comparisons below). For putative new species 2 from Deqin County, it is morphologically most similar to *D. vela*, but it can be differentiated from the latter species by the presence of distinct gular spots in both sexes (vs. absence), weaker, discontinuous vertebral crest in males (vs. strongly developed and continuous), and an true allopatric, isolated distribution (Jinsha River Valley for putative new species 2 vs. Mekong River Valley for *D. vela*; two valleys are separated by snow mountains over 4000m of elevation; Fig. 1).

Molecular Results

Similar to previous studies, all analyses supported the monophyly of the genus *Diploderma* with strong support (Clade A, ML bootstrap support [BS] 100/Bayesian posterior probability [PP] 1.00; support values presented in this order hereon), and two major clades, namely Clade B and Clade C were recovered within the genus *Diploderma*. The *D. flaviceps* complex is again supported as paraphyletic, with the true *D. flaviceps* recovered within Clade B, sister to *D. splendidum* (99/1.00), while most species of the complex, including the two putative new species, are recovered within Clade C, paraphyletic with respect to true *D. flaviceps* (Fig. 2).

Within Clade C, although relationships are not fully resolved, key nodes that demonstrate the paraphyletic nature between putative new species and their morphologically similar congeners are well supported. Specifically, the two putative new species, *D. angustelinea*, *D. aorun*, *D. batangense*, *D. brevicaudum*, *D. drukdaypo*, *D. panchi*, *D. qilin*, *D. vela*, and *D. yulongense* form Clade D (70/0.96), with putative new species 1 being sister to the rest of the clade, followed by *D. batangense* with moderate supports (Clade E, 57/0.98). Remaining species of Clade D form another well-supported subclade (Clade F, 76/1.00). *Diploderma brevicaudum* is sister to *D. qilin* with strong support (99/1.00). *Diploderma vela* is sister to *D. drukdaypo* (91/0.94), and together with putative new species 2, they form a well-supported sub-clade (Clade H, 94/1.00).

Both putative new species are genetically divergent from true *D. flaviceps*, with the uncorrected genetic distance ranging from 17.7–19.8% (Table 1). For putative new species 1, the divergence is 8.7–9.3% from its morphologically similar congener *D. angustelinea*. For putative new species 2, the divergence is 2.8–3.3% and 3.2–3.4% to *D. drukdaypo* and *D. vela*, respectively (Table 3).

Although the genetic distances between putative new species 2 and its morphologically similar species (*D. drukdaypo* and *D. vela*) are low, the putative new species 2 is monophyletic, and it possess diagnostic gular coloration and a true allopatric distribution (separated by snow mountains) with respect to latter two recognized species. As both distinct gular coloration and allopatric distribution across HMR have been suggested to create reproductive isolation through sexual selection (Wang *et al.* 2016, 2020b; Stuart-Fox & Ord 2004) and geographic isolation (Wang *et al.* 2015; Dong *et al.* 2020), respectively, it is clear that the second putative new species represent a recently diverged lineage that is distinct evolutionarily from its closely related congeners.

Therefore, combining genetic, morphological, as well as allopatric distribution data, and we describe the two populations of *D. cf. flaviceps* from Muli County and Deqin County as two new species. Additionally, we confirm the newly collected specimens from Lijiang and nearby areas are *D. brevicaudum*, which represent the rediscovery of the species in the wild at the first time.

Taxonomic Accounts

Diploderma brevicaudum (Manthey, Denzer, Hou, Wang, 2012)

(Figure 3–5; Table 2)

Holotype: AMNH 19879, adult male. Collected by R. C. Andrews and Edmund Heller from Snow Mt. Village (27.083° N, 100.183° E; the precision is as reported originally by Manthey *et al.* 2012), 19km north of Lijiang, Yunnan, China in November 1916.

Paratypes: ZMB 28932, adult female, collected by Camillo Schneider from area near Lijiang, Yunnan, China (26.883° N, 100.183° E) in October 1914; AMNH 19878, adult female, collected by R. C. Andrew and Edmund Heller on a mountain overlooking Lijiang on 11 October 1916; NMW 20853, juvenile, collected by Heinrich Freiherr von Handel-Mazzetti from Lijiang in June 1915.

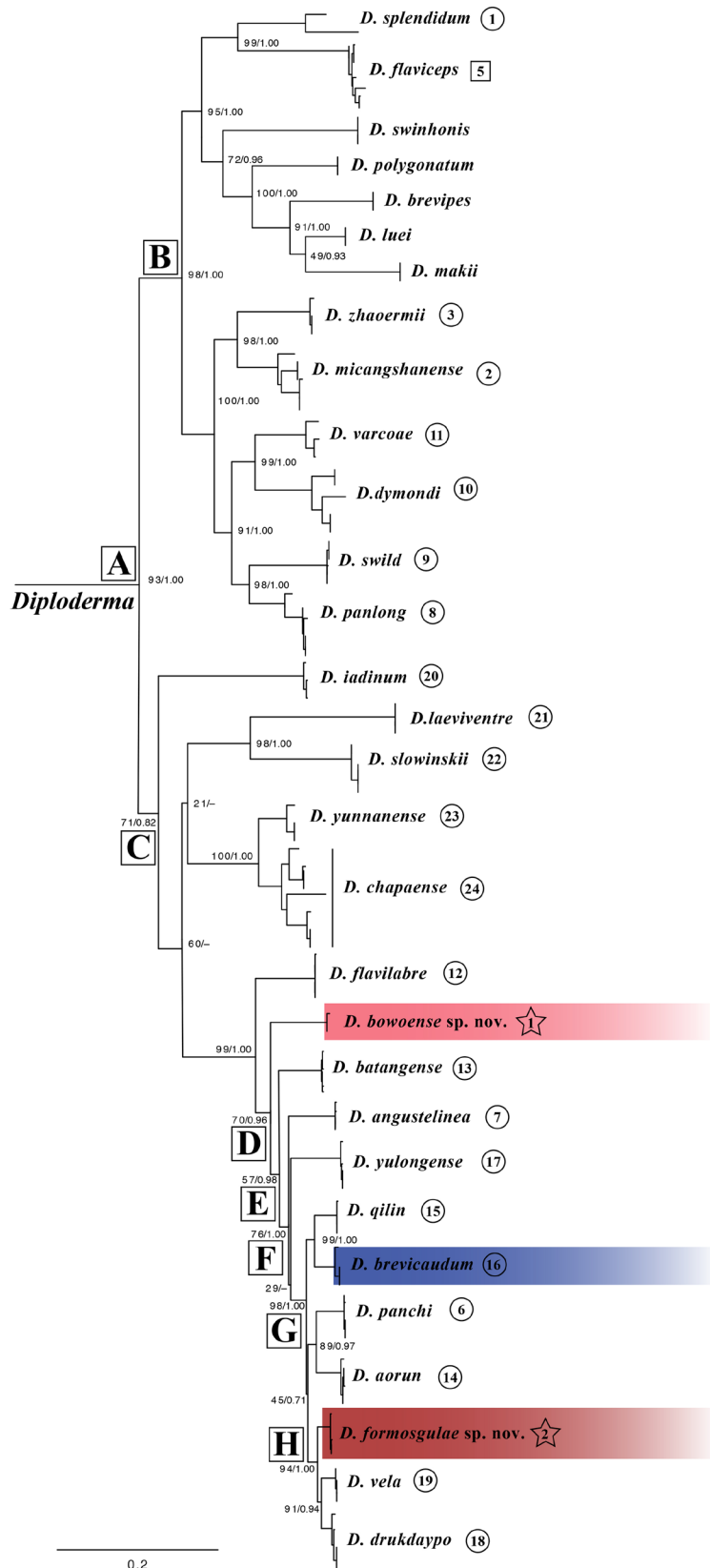


FIGURE 2. Phylogenetic relationships among members of the genus *Diploderma* inferred from mitochondrial gene *ND2* (1031bp). Bayesian posterior probabilities are mapped onto the topology from Maximum Likelihood analyses. All tip nodes that unify each individual species are well supported (BS \geq 90, BP \geq 0.98) and hence removed from the tree. “–” indicates unresolved relationships at the node in question in Bayesian analyses. The two new species and *D. brevicaudum* are shaded with the same color as they appear in the map in Figure 1. The circled number of each species corresponds to those presented in Figure 1.

Newly collected specimens: KIZ 044497, adult male, from the Developing District of Lijiang, 20km northwest from Lijiang City, Yunnan, China (27.035° N, 100.064° E, WGS 84, elevation 1854m); KIZ 044305, adult female, KIZ 044306, adult male, both from the mountain overseeing Lijiang City, Yunnan, China (26.949° N, 100.199° E, WGS 84, elevation 2692m); all collected by Kai Wang, Zhuoyu Lu, Man Fu, and Xiankun Huang on 10 June 2019. KIZ 028338, adult female from Shangjiang Village, Shangrila County, Yunnan, China (27.372° N, 99.665° E, elevation 2152m), collected by Kai Wang and Jinlong Ren on 10 June, 2016.

Expanded diagnosis: *Diploderma brevicaudum* can be differentiated from congeners by a combination of the following characters: (1) small to medium size, SVL 48.0–57.2mm in males, 60.0–65.2mm in females; (2) tail length moderate in males (TAL 140–184.1% SVL), short in females (125.0–159.1%); (3) head moderate in shape, HW 68.5–74.8% HL, HD 70.2–74.4% HW; (4) limbs length moderate, FLL 33–48.7% SVL, HLL 60–80.7%; (5) tympanum concealed; (6) transverse gular fold present, distinct; (7) T4S 16–23; (8) MD 34–43; (9) black radial stripes limited to superior and posterior portion of eyes; (10) dorsolateral stripes present in all males, moderately jagged, Pale Sulphur Yellow [Color 92], sometimes in females, same color as in males but much paler; (11) gular spot present in males only, Pale Sulphur Yellow [Color 92]; and (12) inner lips Sulphur Yellow [Color 80], tongue Light Orange Yellow [Color 77], remaining oral cavity mostly Light Flesh Color [Color 250] (Table 3).

Expanded comparisons against morphologically similar congeners: *Diploderma brevicaudum* is similar morphologically and most closely related to *D. qilin*, in which both species have similar brownish dorsal body coloration and similar gular spot coloration in males (Light Sulphur Yellow [Color 93]). Additionally, both species are distributed along the upper Jinsha River close to each other. However, *D. brevicaudum* can be differentiated from *D. qilin* by having a shorter tail, particularly in females (TAL 140–184.1% SVL in males, 125.0–159.1% in females vs. 201.0–218.2% in males, 174.3–199.7% in females), a distinct inner lip and tongue coloration (inner lips Sulphur Yellow [Color 80], tongue Light Orange Yellow [Color 77] vs. both inner lips and tongue Light Flesh Color [Color 250]), and by the absence of gular spots in females (vs. presence).

Diploderma brevicaudum is also morphologically similar to *D. drukdaypo* and *D. flavilabre*, in which all three species have relatively short tails, and both *D. brevicaudum* and *D. flavilabre* have yellowish colored inner lips. However, *D. brevicaudum* can be differentiated from the two congeners by having Light Sulphur Yellow [Color 93] gular spots in males only (vs. absence in both sexes of *D. drukdaypo*, Pale Emerald Green [Color 141] to Light Turquoise Green [Color 146] in both sexes of *D. flavilabre*). Furthermore, *D. brevicaudum* differs from *D. drukdaypo* by having distinctively keeled ventral body and head scales (vs. feebly keeled or smooth) and a distinct inner lip and tongue coloration (inner lips Sulphur Yellow [Color 80], tongue Light Orange Yellow [Color 77] vs. both inner lips and tongue Light Flesh Color [Color 250]); and from *D. flavilabre* by having distinctively keeled ventral head scales (vs. feebly keeled) and by a distinct tongue coloration (Light Orange Yellow [Color 77] vs. Light Flesh Color [Color 250]).

Diploderma brevicaudum is distributed closely with *D. yulongense*, but it can be differentiated from *D. yulongense* by having a relatively shorter tail (TAL 140–184.1% SVL in males, 125.0–159.1% in females vs. 193.7–244.3% in males, 182.2–211.3% in females), a distinct gular coloration (present in males only, Light Sulphur Yellow [Color 93] vs. present in both sexes, Opaline Green [Color 106]), and a distinct inner lip and tongue coloration (inner lips Sulphur Yellow [Color 80], tongue Light Orange Yellow [Color 77] vs. both inner lips and tongue Light Flesh Color [Color 250]).

Coloration in life based on newly collected specimens (Figs. 3 and 4). In males, the dorsal surface of head is Cinnamon-Drab [Color 50] to pale Drab [Color 19]. Two Clay Color [Color 18] to Brunt Umber [Color 48], narrow transverse streaks are present between orbits on the dorsal surface of head. Sometimes the two transverse streaks are connected via a narrow lateral streak, which is the same color as the transverse ones. The two transverse streaks on the dorsal surface of the head enter the orbit laterally on each side, forming the superior parts of the dark radial stripes around eyes. An additional Brunt Umber [Color 48], thicker streak is present from the postero-inferior corner of eye to the corner of mouth on each side. No additional radial stripes are present inferior to the eyes, and a Light Buff [Color 2] to Cream Color [12] lip-stripe is present inferior to the eyes from the nasal scale to the axis of jaw on each side.

The dorsal body is Amber [Color 51] in background. Two Light Yellow Ocher [Color 13] to pale Sulphur Yellow [Color 80], jagged dorsolateral stripes are present from the neck to the pelvis on each side of the body. Five to Six Brunt Umber [Color 48], triangular patches are evenly distributed along the vertebral line between the dorsolateral stripes from the neck to the base of the tail, all of which pointing posteriorly. The dorsal color of Amber [Color 51]

transitions sharply into Drab [Color 19] on ventrolateral sides. Dorsal surfaces of the limbs are pale Drab [Color 19] with numerous somewhat faint Army Brown [Color 46] transverse bands. Faint Army Brown [Color 46] transverse bands are also present on the tail, which are slightly more distinct toward the posterior portion.

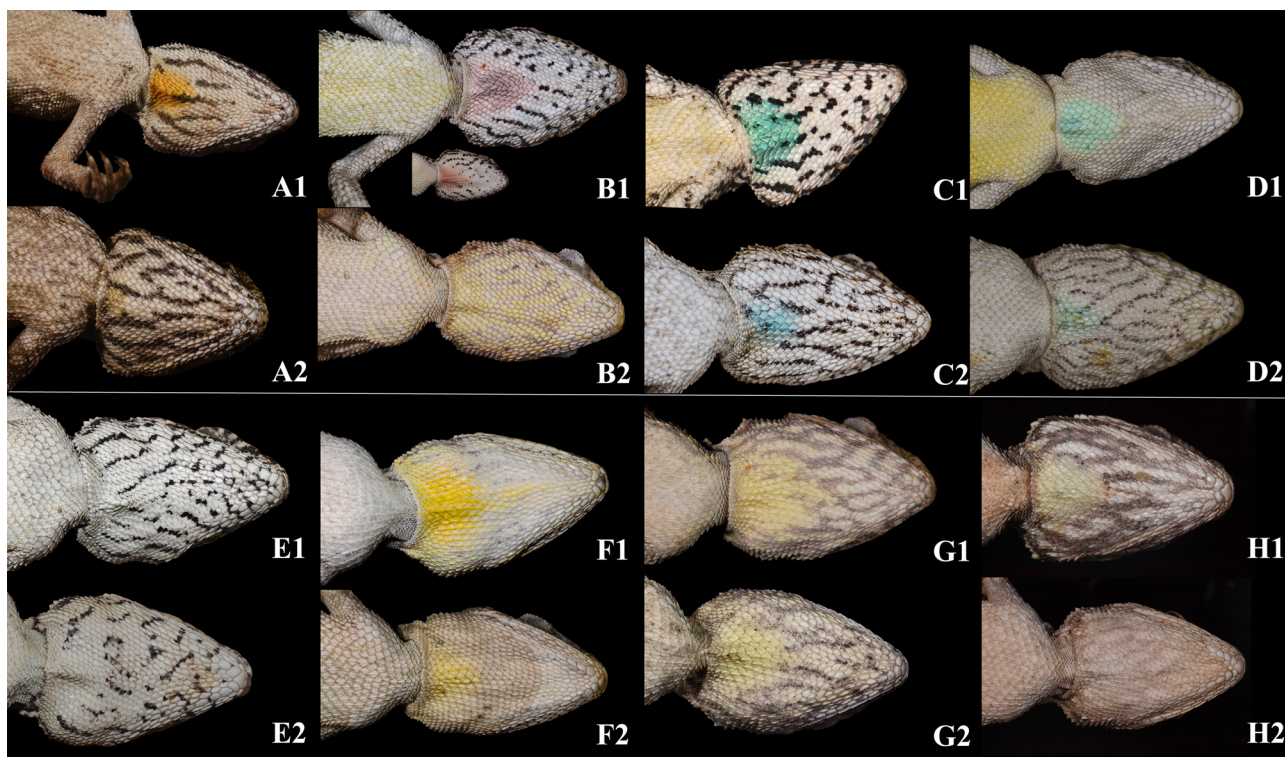


FIGURE 3. Comparisons of gular coloration in life between (1) males and (2) females of (A) *Diploderma bowoense* sp. nov., (B) *D. formosugulae* sp. nov., (C) *D. aorun*, (D) *D. batangense*, (E) *D. vela*, (F) *D. angustelinea*, (G) *D. qilin*, and (H) *D. brevicaudum*. The smaller inset photos in A1 represent gular coloration of the representation of juvenile male of *D. formosugulae* sp. nov. Photos by Kai Wang.

The background coloration of the ventral surface of the head is pale Drab [Color 19]. White to Light Buff [Color 2] streaks and patches are scattered on the ventral surface of the head, embellishing the background drab color into a reticulated pattern. A triangular, Light Sulphur Yellow [Color 93] gular spot is present on the posterior central part. The ventral surface of the body is uniform Pale Pinkish Buff [Color 3] to Flesh Color [Color 249]. Ventral surfaces of the limbs are tail are uniform Light Buff [Color 2]. The inner lips are Sulphur Yellow [Color 80], whereas the tongue is Light Orange Yellow [Color 77]. Remaining parts of the oral cavity are mostly Light Flesh Color [Color 250].

In females, the coloration and ornamentation differ from the males. Specifically, the dorsal and lateral background coloration is Drab [Color 19]; the dorsolateral stripes on the body are more narrower and less distinct; the ventral surface of the head is uniform white to Light Buff [Color 2] without dark reticulated patterns or gular spot; and the ventral surface of the body is uniform white or Light Buff [Color 2].

Natural history and conservation. *Diploderma brevicaudum* inhabits mixed forests at mid-elevation (1854–2740m). Currently, the species is known only from Lijiang and nearby Shangrila County in Yunnan Province, China, and the estimated area of occurrence is about 4000km². Although living in forest habitat, the species is terrestrial for the most part, basking on rock piles at the base of tree trunks in open areas during the day, and sleeping on twigs of bushes at night. Unlike all remaining species in the HMR, both males and females of *D. brevicaudum* are very aggressive when captured, hissing and displaying their yellow oral cavities as threat signals. Several other reptile species were observed to occur in sympatry at the site of observation, including *Ptyas nigromarginata*, *Gloydus monticola*, *Protobothrops jerdoni*, *Scincella monticola*, and *Gekko scabridus*.

Based on our surveys and interviews with local communities, the population density of *D. brevicaudum* is much lower than other congeners in the nearby regions of the HMR (i.e. *D. yulongense* and *D. qilin*). Habitat destruction is the main threat to the species based on our surveys, resulting from illegal mining, tourism-related infrastructure

development, and the continued growth of Lijiang City. According to IUCN criteria B1 a and b (iii and v), *D. brevicaudum* meets the classification status of Endangered (EN), and should be added to the list of Class II species protected in the Endangered Species List in China.

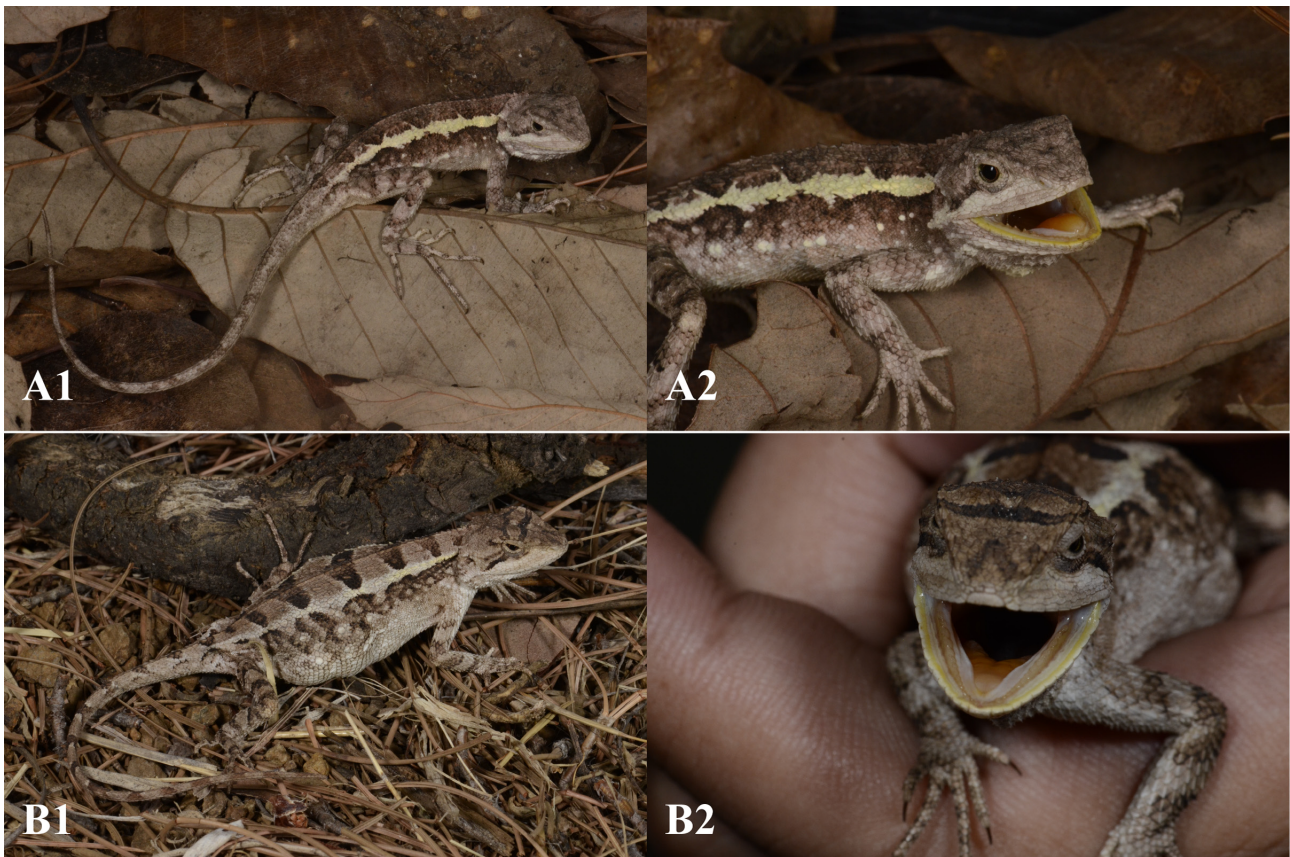


FIGURE 4. Dorsolateral view (1) and closeup of oral characteristics (2) of the male KIZ 044497 (A) and female KIZ 044305 (B) of *Diploderma brevicaudum* in life. Photos by Kai Wang.

***Diploderma bowoense* sp. nov. Wang, Gao, Wu, Siler, Che**

(Figs. 3, 6, 7, 8, and 11; Table 4)

LSID urn:lsid:zoobank.org:act:DC266DAA-E8C2-4BB7-84D3-469361331F42

Chresonyms. *Japalura flaviceps* Zhao & Yang 1997: 165–167; Zhao *et al.* (1999: 111–115), in part; Zhao (2004): 84.

Holotype. KIZ 044700, adult male, from Bowo Village, Muli Tibetan Autonomous County, Sichuan Province, China (101.1569° E, 28.8098° N, elevation 2328m, WGS 84). Collected by Kai Wang, Zhuoyu Lu, Zhongyang Cireng, and Xiankun Huang on 25 June 2019.

Paratypes. KIZ 044701, adult male; KIZ 044703, 044756, adult females; All share the same collection information as the holotype.

Etymology. The Latin species epithet, *bowoense*, is derived from the Tibetan name of the type locality of the new species. We name the new species using the Tibetan name for the type locality in honoring the positive conservation influence of Tibetan culture on the habitats and the inhabiting wildlife at the type locality. We suggest Bowo Mountain Dragon as its English common name, and 博窝龙蜥 (Pinyin: Bo Wo Long Xi) as its Chinese common name.

Diagnosis. The new species can be diagnosed based on a combination of the following morphological characters: 1) body size small, SVL 45.7–53.7 mm in males, 52.6–54.2mm in females; 2) tail length moderate, TAL 189.1–201.9% SVL in males, 177.3–178.7% in females; 3) HW 65.1–70.5% HL; 4) HLL 72.6–78.6% SVL; 5) nuchal and dorsal crests moderately developed on weak skin folds in males; 6) distinct transverse gular fold present; 7) tympanum concealed; 8) MD 40–44; 9) F4S 15–17; 10) T4S 19–21; 11) PTS 3 or 4; 12) PTY 3–7; 13) PRS 3–6;

14) dorsolateral stripes strongly jagged, Cream Color [Color 12] in males, Sulphur Yellow [Color 80] and faint in females; 15) gular spots present in both sexes, smaller in females, Light Chrome Orange [Color 76] in live males, Dark Spectrum Yellow [Color 78] in live females, absent after preservation; 16) inner lips, oral cavity, and tongue all Light Flesh Color [Color 250]; and 17) distinct vermiculate stripes present on ventral surface of the head.



FIGURE 5. Micro- and macro-habitat for *Diploderma brevicaudum* at the type locality in the mountains overseeing Lijiang City (near Wenhai), Yunnan, China. Photos by Zhuoyu Lu.

Comparisons. Previously, the new species had been confused with *D. flaviceps*, but can be differentiated by having a smaller body size in males (SVL 45.7–53.7mm vs. 68.5–82.1mm), weak skin folds under both dorsal and nuchal crests in males, absence in females (vs. strongly developed and erected in males, presence in females), and by the presence of distinct radial stripes around the eyes (vs. absence), absence of a lateral series of dark, hollow

rhomboid patterns between dorsolateral stripes on the dorsum (vs. presence), and by the presence of colorful gular spots in both sexes (vs. absence).

In comparison with species distributed in close proximity and along the same upper Yalong River, *D. bowoense* **sp. nov.** differs from *D. angustelina* by having a shorter tail (TAL 189.1–201.9% SVL in males, 177.3–178.7% in females vs. 230.2–249.1% in males, 194.30–222.3% in females; Fig. 6), better developed nuchal and dorsal crest with weak skin folds in males (vs. feeble crests with no skin folds), and by the presence of distinct dark vermiculate stripes on the ventral surface of the head in both sexes (vs. absence or faint); from *D. panchi* by having a longer tail (TAL 177.3–178.7% SVL in females vs. 141.8–151.5% in females; Fig. 6), and by a distinct gular pattern in females (distinct Dark Spectrum Yellow [Color 78] gular spot vs. mosaic Light Sulphur Yellow [Color 93] patterns); and from *D. panlong* by having a much smaller body size in males (SVL 45.7–53.7mm vs. 60.2–71.7mm), a concealed tympanum (vs. exposed in most individuals), different coloration of the oral cavity and tongue (Light Flesh Color [Color 250] vs. oral cavity Dark Spectrum Yellow [Color 78], tongue Light Chrome Orange [Color 76]), and by the presence of gular spots in males (vs. absence).

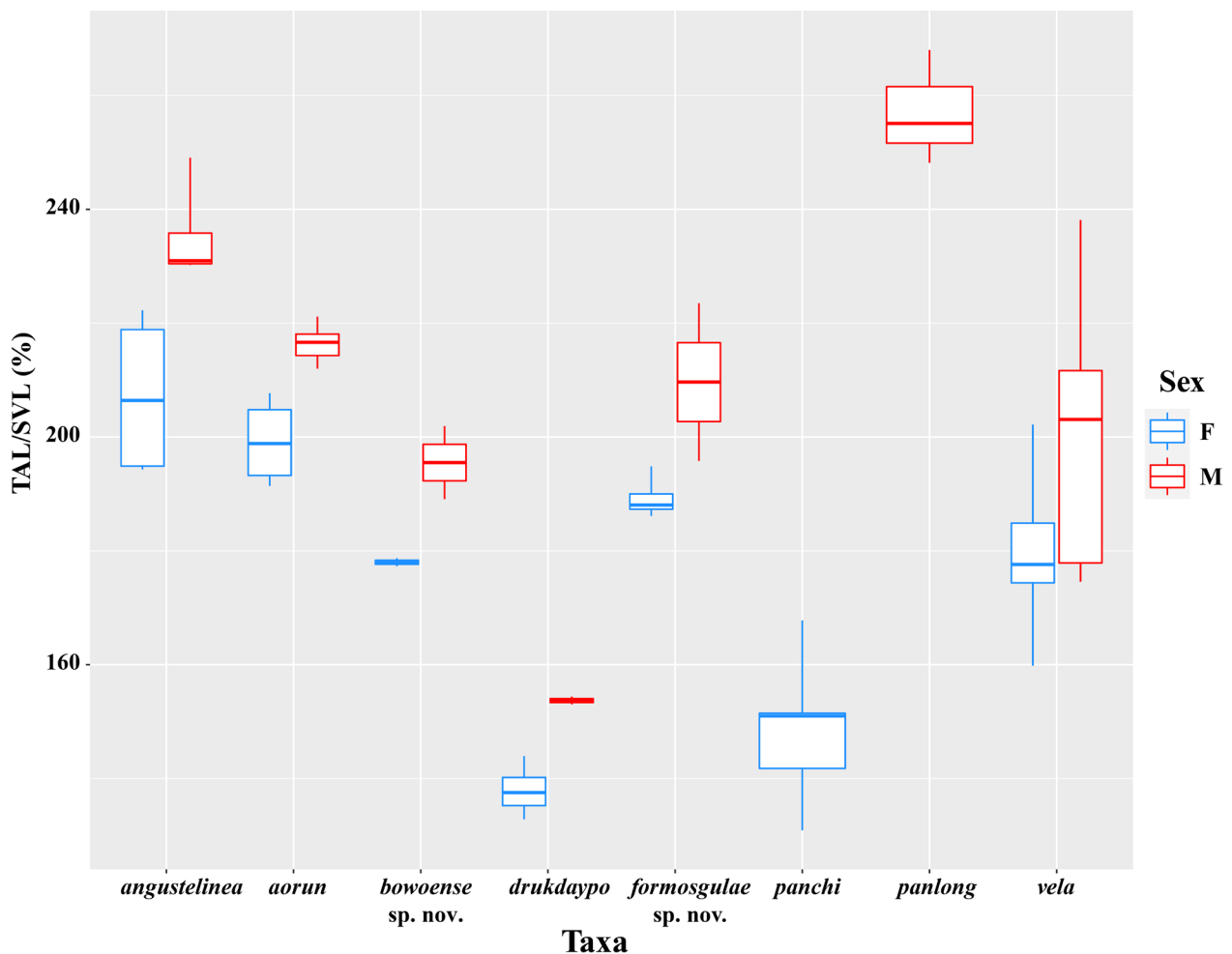


FIGURE 6. Boxplot showing the important diagnostic morphometric character, relative tail length, of males and females of the two new species (*Diploderma bowoense* **sp. nov.** and *D. formosgulae* **sp. nov.**) and their closest congeners. Each box represents the interquartile range (25th to 75th percentile), the thick horizontal bar inside each box indicates the median value, the vertical lines indicate maximum and minimum values. *Diploderma panchi* and *D. panlong* are known by a single sex only (female and male, respectively), therefore data of only one sex are available.

From all three species distributed along the upper Mekong River Valley (i.e. *D. drukdaypo*, *D. iadinum*, and *D. vela*), *D. bowoense* **sp. nov.** can be differentiated from all three species by the presence of a distinct coloration of gular spots (Light Chrome Orange [Color 76] in males, Dark Spectrum Yellow [Color 78] in females vs. absence in *D. drukdaypo* and *D. vela*; Caribbean Blue [Color 168] in males, Medium Greenish Yellow [Color 88] in females of *D. iadinum*). Additionally, *D. bowoense* **sp. nov.** differs from *D. drukdaypo* by having distinctively keeled ventral

scales of head and body (vs. smooth or feebly keeled) and a much longer tail (TAL 189.1–201.9% SVL in males, 177.3–178.7% in females vs. 153.0–154.4% in males, 132.8–144.0% in females); from *D. iadinum* by having a distinct body coloration and ornamentation in males (Jet Black [Color 300] to Raw Umber [Color 22] in background, with Cream Color [Color 12], strongly jagged dorsolateral stripes in males vs. Yellowish Spectrum Green [Color 128] to Emerald Green [Color 143] background coloration, with same colored, smooth-edged dorsolateral stripes) and by the absence of multiple regular lateral rows of enlarged scales on the dorsum (vs. presence); and from *D. vela* by the absence of strongly developed, continuous sail under the vertebral crests in males (vs. feeble).

From all species distributed along the upper Jinsha River (*D. aorun*, *D. batangense*, *D. brevicaudum*, *D. flavilabre*, *D. qilin*, and *D. yulongense*), *D. bowoense* **sp. nov.** differs by having a distinct coloration of gular spots in both sexes (Light Chrome Orange [Color 76] in males, Dark Spectrum Yellow [Color 78] in females vs. Pale Cyan [Color 157] to Light Caribbean Blue [Color 163] in both sexes of *D. aorun*; Pale Cyan [Color 157] in both sexes of *D. batangense*; Pale Sulphur Yellow [Color 92] in males only of *D. brevicaudum*; Pale Emerald Green [Color 141] to Light Turquoise Green [Color 146] in both sexes of *D. flavilabre*; Light Sulphur Yellow [Color 93] in both sexes of *D. qilin*; and Chartreuse [Color 89] to Opaline Green [Color 106] in both sexes of *D. yulongense*). Additionally, *D. bowoense* **sp. nov.** differs from *D. aorun* by having a shorter tail (189.1–201.9% SVL in males, 177.3–178.7% in females vs. 212.0–221.1% in males, 191.4–207.7% in females); from *D. brevicaudum* and *D. flavilabre* by having a longer tail (189.1–201.9% SVL in males, 177.3–178.7% in females vs. 184.1–188.7% in males, 136.8–159.1% in females in *D. brevicaudum*; 149.7–179.3% SVL in males, 140.2–152.2% in females in *D. flavilabre*) and by distinct inner lip and tongue coloration (Light Flesh Color [Color 250] vs. inner lips Sulphur Yellow [Color 80], tongue Light Orange Yellow [Color 77] in *D. brevicaudum*; inner lips Dark Spectrum Yellow [Color 78] in *D. flavilabre*); from *D. qilin* by having a smaller body size in males (SVL 45.7–53.7mm vs. 55.9–66.5mm); and from *D. yulongense* by having a shorter tail in females (TAL 177.3–178.7% SVL vs. 182.1–211.3%).

Compared to both species distributed along the upper Salween River (*D. laeiventre* and *D. slowinskii*), *D. bowoense* **sp. nov.** differs from *D. laeiventre* by having fewer MD (MD 40–44 vs. 57–59) and distinctively keeled ventral scales (vs. smooth or feebly keeled); and from *D. slowinskii* by having concealed tympana (vs. exposed) and a much smaller body size (SVL 45.7–53.7mm in males, 52.6–54.2mm in females vs. >74mm).

Finally, *D. bowoense* **sp. nov.** can be differentiated from *D. chapaense*, *D. fasciatum*, *D. micangshanense*, *D. menghaiense*, *D. varcoae*, *D. yunnanense*, and all species from East Asian Islands (*D. brevipes*, *D. luei*, *D. makii*, *D. polygonatum*, and *D. swinhonis*) by the presence of a distinct transverse gular fold (vs. absence); from *D. dymondi* and *D. swild* by having concealed tympana (vs. exposed); from *D. splendidum* by having strongly jagged dorsolateral stripes in males (vs. smooth edged) and homogeneous scales on the ventral surface of the head (vs. heterogeneous); from *D. hamptoni* by having parallel, jagged dorsolateral stripes (vs. diagonally away from midline and smooth); and from *D. zhaoermii* by having distinct coloration of gular spots in both sexes (Light Chrome Orange [Color 76] in males, Dark Spectrum Yellow [Color 78] in females vs. Chartreuse [Color 89] in males, no gular spots in females) and by having a much smaller body size (SVL 45.7–53.7mm in males, 52.6–54.2mm in females vs. 63.2–81.7mm in males, 61.0–75.2mm in females).

Description of holotype. Body not dorsally compressed, SVL 53.7mm; tail long, TAL 201.9% SVL; limbs length moderate, FLL 45.2% SVL, HLL 75.6% SVL; head shape moderate, HW 65.1% HL, HD 75.7% HW; SEL 39.5% HL. Rostral rectangular, three times wider than height, two scales away from nasal; nasal oval, somewhat elongated, two scales away from first supralabial; supralabials 10/10, last one longest, weakly keeled; infralabials 10/12, less keeled than supralabials; suborbital scale rows 3/3, each scale bearing distinct, lateral keel; supraciliaries 8/8, overlapping one half of total length with succeeding ones; enlarged, protruding scales between posterior orbit and tympanum, 7/8, each bearing single distinct, lateral keel; tympanum concealed under fine scales; post tympanic conical scales 5/7, moderately developed; enlarged post-riotal scales 3/3, sub-pyramidal in shape. Dorsal head scales heterogeneous in size and shape, all distinctively keeled; single, laterally oriented, Y-shaped ridge present on dorsal snout, starting two scales posterior of rostral to anterior end of orbit; interparietal large, parietal eye distinct; postciliary scale much enlarged, subpyramidal shape; post occipital conical scales moderately differentiated, 3/3.

Dorsal body scales distinctively keeled, heterogeneous in size and shape; axillary scales fine; shoulder fold present, distinct, extending posteriorly over axilla; enlarged scales arranged in two dorsolateral rows on each side of dorsum from neck to pelvis, ones close to dorsal midline, one along mid-dorsolateral stripe; nuchal, dorsal crests well developed on rather weak skin folds, crest scales erected, serrated, differentiated from nearby dorsal scales; mid-dorsal scales 44. Scales of dorsal limbs distinctively keeled, distinctively heterogeneous on hind limbs; Finger IV and Toe IV longest, Finger IV subdigital lamellae 17/16, Toe IV subdigital lamellae 21/21.

Ventral head scales homogeneous in size and shape, distinctively keeled except chin shields; mental pentagonal, completely enclosed by first pair of chin shields; chin shields 7/7, smooth, two scale rows away from infralabials. Gular pouch present, well developed in life, indistinct after preservation; distinct transverse gular fold present, deep. Ventral body and limb scales distinctively keeled, more pronounced than those of ventral head, homogeneous in size and shape, keel of individual scale mostly regularly arranged in lateral rows.

Coloration. The background coloration of the dorsal and lateral surface of the head is Drab Gray [Color 256] to pale Dark Neutral Gray [Color 299]. Four Sepia [Color 286] to Jet Black [Color 300] transverse ornamentation patterns are present on the dorsal surface of head: the first streak is at the posterior edge of the orbit, the second streak is between the anterior edge of the orbit, the third streak is an X-shaped pattern at the midpoint between the eyes and nares, and the last streak is between the nares. Dark Neutral Gray [Color 299] or Jet Black [Color 300] streaks form the radial stripe pattern around the eye, many of which are vague and not clearly defined. A white lip stripe is present in the suborbital region, although the anterior one-third of the stripe is heterogeneous in color and speckled with Medium Neutral Gray [Color 298].

The background coloration of the dorsum is Drab [Color 19] to Dark Neutral Gray [Color 299]. A Sepia [Color 286] to Jet Black [Color 300] reticulated ornamentation pattern is present on the lateral surface of the body inferior to the dorsolateral stripes. A dorsolateral stripe is present on each side of the vertebral crest on the dorsum, running from the neck to the pelvis. The stripe is strongly jagged, with five rhombus-shaped extensions distributed evenly across the stripe from the shoulder to the pelvis. Dorsolateral stripes are Cream Color [Color 12] with irregular and faded speckles of Olive Horn Color [Color 16]. The nuchal and dorsal crests are Clay Color [Color 18] and distinct from the rest of the dorsal surface coloration. The dorsal surfaces of the limbs and tail are Drag Gray [Color 256], with evenly distributed Dark Neutral Gray [Color 299] transverse bands or streaks running from the proximal to distal ends. The streaks get paler towards the distal ends of the fingers, toes, and the tip of the tail.

The ventral surface of the head is Light Buff [Color 2], with Jet Black [Color 300] short streaks, which are formed by 2–3 rows of black scales. A distinct, Light Chrome Orange [Color 76], triangular-shaped gular spot is present at the center of the gular region. The ventral surfaces of the body, limbs, and tail are uniform Light Buff [Color 2].



FIGURE 7. Dorsolateral view (1) and closeup of the lateral surface of the head (2) of the male holotype KIZ 044700 (A) and female paratype KIZ 044703 (B) of *Diploderma bowoense* **sp. nov.** in life. Photos by Kai Wang.

Variation. Detailed morphological variation is summarized in Table 4. The paratype male (KIZ 044701) has a shorter tail than the holotype, and the Clay Color [Color 18] of nuchal and dorsal crests are indistinct. Sexual dimorphism is evident despite the small sample size, with males possessing relatively longer tails, relatively shorter trunks, and taller nuchal crests (Table 4). Furthermore, similar to most *Diploderma* congeners, *D. bowoense* **sp. nov.** are sexually dichromatic, where males have different gular coloration than females. In females, the gular spots are less saturated, and the color is Dark Spectrum Yellow [Color 78]. Between the two females, only one (KIZ 044703) has a similar vertebral stripe as is observed on the male holotype, and the coloration is more saturated (Cinnamon-Rufous [Color 31] to Light Pratt's Rufous [Color 71]) than the holotype. The other female has six Dark Neutral Gray [Color 299], reverse triangle-shaped blotches scattered evenly along the vertebral line from the neck to the pelvis.

Natural history and conservation. *Diploderma bowoense* **sp. nov.** inhabits hot-dry valleys along the middle Yalong River in Muli County, Sichuan Province, China. Currently, the species is known only from the type locality near Bowo Village, but it is likely to be found further northward along the Yalong River Valley. Individuals were found active during the day, basking on rock piles and open ground, but slept on tall bushes at night. *Amolops mantzorum*, *Elaphe carinata*, and *E. taeniura* were found at the type locality of *D. bowoense* **sp. nov.**. Although the habitats at the type locality are well protected thanks to the local Tibetan community, the remaining habitat of the species along the main Valley of Yalong River are still threatened by the ongoing development of a nearby hydropower station. We recommend Data Deficient (DD) for the IUCN status of *D. bowoense* **sp. nov.** and call for ecological and population studies of the new species in the future.

***Diploderma formosgulae* sp. nov. Wang, Gao, Wu, Dong, Shi, Qi, Siler, Che**

(Figs. 3, 6, 8–10; Table 4)

LSID urn:lsid:zoobank.org:act:82CF4E0B-91B6-426B-9F4C-1008BE514F06

Chresonyms. *Japalura flaviceps* Zhao & Yang 1997:165–167; Zhao *et al.* 1999:111–115; Yang & Rao 2008:200.

Holotype. KIZ 044425, adult male, from Yangla Village, Deqin County, Yunnan Province, China (99.1113° E, 28.8905° N, elevation 2355m, WGS 84). Collected by Kai Wang, Zhuoyu Lu, Man Fu, and Xiankun Huang on 17 June 2019.

Paratypes. KIZ 044373, 044417, adult males; KIZ 044418, subadult male; KIZ 044424, 044427, 044428, 044435, juvenile males; KIZ 044375, 044420, 044421, 044423, adult females; KIZ 044429, 044430, 044437, juvenile females. All share the same collection information as the holotype.

Etymology. The Latin species epithet *formosgulae* means “beautiful gular”, which describe the vibrant and diagnostic gular spots of the species. We suggest Vibrant-gulared Mountain Dragon as its English common name, and 丽喉龙蜥 (Pinyin: Li Hou Long Xi) as its Chinese common name.

Diagnosis. The new species can be diagnosed based on a combination of the following morphological characters: 1) body size moderate, SVL 55.5–60.9 mm in males, 55.9–60.2mm in females; 2) tail long, TAL 195.8–223.5% SVL in males, 186.1–194.8% in females; 3) HW 66.2–75.4% HL; 4) HLL 73.0–80.3% SVL; 5) nuchal and dorsal crests developed on moderate skin folds in males; 6) MD 37–48; 7) F4S 13–16; 8) T4S 18–24; 9) PTS 2–4; 10) PTY 3–6; 11) PRS 4–8; 12) subocular regions and chin pale Pink [Color 242] in most individuals; 13) dorsolateral stripes jagged and Cream Color [Color 12] in males, narrow and Sulphur Yellow [Color 80] or indistinct in females; 14) ventral body uniform Pale Pinkish Buff [Color 3] to Pale Sulfur Yellow [Color 92]; 15) gular spots always present in males, Pinkish Flesh Color [Color 253] to Lilac [Color 222], either as Sulphur Yellow [Color 80] gular spots or Sulphur Yellow [Color 80] reticulated stripes in females.

Comparisons. The new species has been confused with *D. flaviceps*, but it can be differentiated by the latter by having a smaller body size in males (SVL 55.5–60.9 mm vs. 68.5–82.1mm) and by the presence of distinct radial stripes around eyes (vs. absence), absence of skin folds under nuchal crests in females (vs. presence), absence of lateral series of dark rhomboid patterns between dorsolateral stripes (vs. presence), and by the presence of colorful gular spots or gular patterns in both sexes (vs. absence).

For species that are phylogenetically closely related but allopatric (*D. drukdaypo* and *D. vela*), *D. formosgulae* **sp. nov.** can be differentiated from the latter two by the presence of colorful gular spots in both sexes (vs. absence in both *D. drukdaypo* and *D. vela*). In addition, the new species differ from *D. drukdaypo* by having distinctively keeled ventral scales of head and body (vs. smooth or feebly keeled) and a much longer tail (TAL 195.8–223.5%

SVL in males, 186.1–194.8% in females vs. 153.0–154.4% in males, 132.8–144.0% in females; Fig. 6); and from *D. vela* by the absence of strongly developed, continuous sail under the vertebral crests in males (vs. presence).

For all remaining recognized species, *D. formosgulae* **sp. nov.** can be differentiated from all species within the HMR (except *D. grahami* and *D. panchi*) by having distinct coloration of gular spots in life (Pinkish Flesh Color [Color 253] to Lilac [Color 222] in males, Sulphur Yellow [Color 80] gular spots or reticulated patterns in females vs. Pale Cyan [Color 157] to Light Caribbean Blue [Color 163] in both sexes of *D. aorun*; Spectrum Yellow [Color 79] to Dark Spectrum Yellow [Color 78] in *D. angustelinea*; Light Cyan [Color 157] in both sexes of *D. batangense*; Light Chrome Orange [Color 76] in males, Dark Spectrum Yellow [Color 78] in females of *D. bowoense* **sp. nov.**; Pale Sulphur Yellow [Color 92] in males, no gular spots in females of *D. brevicaudum*; Pale Emerald Green [Color 141] to Light Turquoise Green [Color 146] in both sexes of *D. flavilabre*; Caribbean Blue [Color 168] in males, Medium Greenish Yellow [Color 88] in females of *D. iadinum*; Light Chrome Orange [Color 76] in both sexes of *D. laeviventre*; no gular spots in *D. panlong*, *D. slowinskii* and *D. swild*; Light Sulphur Yellow [Color 93] in both sexes of *D. qilin*; Chartreuse [Color 89] or Opaline Green [Color 106] in both sexes of *D. yulongense*; and Chartreuse [Color 89] in males, no gular spots in females of *D. zhaoermii*).



FIGURE 8. Dorsolateral (1) and ventral (2) views of the male holotype KIZ 044700 (A) and female paratype KIZ 044703 (B) of *Diploderma bowoense* **sp. nov.** in preservation. Photos by Zhongbing Yu.

In addition to distinct gular coloration, *D. formosgulae* **sp. nov.** differs from *D. angustelinea* by having a shorter tail (TAL 195.8–223.5% SVL in males, 186.1–194.8% in females vs. 230.2–249.1% in males, 194.30–222.3% in females; Fig. 6) and more developed nuchal and dorsal crests in males (vs. feeble); from *D. aorun* by a distinct coloration of subocular region and chin (pale Pink [Color 242] vs. white); from *D. batangense* by having a better developed and more conical scales post rictus (PRS 4–9 vs. 0–3); from *D. bowoense* **sp. nov.** and *D. brevicaudum* by having a tendency toward longer tail in males, much longer in females (TAL 195.8–223.5% SVL in males, 186.1–194.8% in females vs. 189.1–201.9% in males, 177.3–178.7% in females for *D. bowoense* **sp. nov.**; 140–184.1% in males, 125.0–159.1% in females of *D. brevicaudum*; Fig. 6); from *D. iadinum* by having less robust head (HD 66.9–73.4% HW vs. 74.0–79.9%) and distinct body coloration (Light Buff [Color 2] to Pale Pinkish Buff [Color 3] vs. Yellowish Spectrum Green [Color 128] to Emerald Green [Color 143] in males, Buff [Color 5] to [Pale Greenish Yellow [Color 86] in females); from *D. laeviventre* by having distinctively keeled ventral scales of head and body

(vs. smooth or feebly keeled); from *D. slowinskii* and *D. swild* by having concealed tympanum (vs. exposed); from *D. yulongense* by the absence of green patches on ventrolateral body of males (vs. presence) and by having more conical scales post rictus (PRS 4–9 vs. 1–4); from *D. zhaoermii* by having a smaller body size (SVL 55.5–60.9 mm in males, 55.9–60.2 mm in females vs. 63.24–81.7 mm in males, 61.0–75.2 mm in females) and less and scattered dark radial stripes around eyes (vs. more and densely positioned).

For *D. grahami*, which does not have coloration data in life, the new species differ from it by having no granular scales (vs. presence) and by having a distinct transverse gular fold (vs. absence). For *D. panchi* that has similar gular patterns in females, *D. formosgulae* **sp. nov.** differs from *D. panchi* by having a much longer tail (TAL 186.1–194.8% in females vs. 141.8–151.5%).

For the remaining species, *D. formosgulae* **sp. nov.** differs from *D. chapaense*, *D. fasciatum*, *D. menghaiense*, *D. micangshanense*, *D. varcoae*, *D. yunnanense*, and all species from East Asian islands (*D. brevipes*, *D. luei*, *D. makii*, *D. polygonatum*, and *D. swinhonis*) by the presence of a deep transverse gular fold (vs. absence); from *D. dymondi* by having concealed tympana (vs. exposed); from *D. hamptoni* by having parallel dorsolateral stripes in males (vs. diagonally oriented) and by having a much deeper transverse gular fold (vs. feeble).



FIGURE 9. Dorsolateral view (1) and closeup of the lateral surface of the head (2) of the male holotype KIZ 044425 (A) and female paratype KIZ 044375 (B) of *Diploderma formosgulae* **sp. nov.** in life. Photos by Kai Wang.

Description of holotype. Body not dorsally compressed, SVL 60.85 mm; tail long, TAL 195.8% SVL; limbs length moderate, FLL 44.8% SVL, HLL 73.0% SVL; head moderate, HW 72.1% HL, HD 72.6% HW; SEL 38.7% HL. Rostral rectangular, twice wider than height, two scales away from nasal; nasal oval, single scale away from first supralabial; supralabials 10/10, weakly keeled, more distinct on last six; infralabials 11/11, feebly keeled, less distinct than supralabials; suborbital scale rows 3/3, each scale bearing distinct, lateral keel; supraciliaries 7/7, overlapping one half of total length with succeeding ones; enlarged, protruding scales between posterior orbit and tympanum, 6/6, each bearing single distinct, lateral keel; tympanum concealed under fine scales; post tympanic conical scales 6/5, well developed and enlarged, two of which much taller than others on each side; enlarged post-rictal scales 4/4, sub-pyramidal in shape. Dorsal head scales heterogeneous in size and shape, all distinctively keeled; single, laterally oriented, Y-shaped ridge present on dorsal snout, starting three scales posterior of rostral to posterior end of orbit; interparietal small, parietal eye distinct; postciliary scale much enlarged, subpyramidal shape, with multiple keels; post occipital conical scales well differentiated, 3/3.

Dorsal body scales distinctively keeled, heterogeneous in size and shape; axillary scales fine; shoulder fold present, distinct, extending posteriorly over axilla; enlarged scales arranged in three dorsolateral rows on each side of dorsum from neck to pelvis, ones close to dorsal midline, and two along dorsolateral stripe; nuchal, dorsal crests well developed on moderate skin folds, crest scales erected, serrated, differentiated from nearby dorsal scales; mid-dorsal scales 43. Scales of dorsal limbs distinctively keeled, distinctively heterogeneous on hind limbs; Finger IV and Toe IV longest, Finger IV subdigital lamellae 14/14, Toe IV subdigital lamellae 18/19.

Ventral head scales mostly homogeneous in size and shape, distinctively keeled except chin shields; mental pentagonal, completely enclosed by first pair of chin shields; chin shields 6/5, smooth, two scale-row away from infralabials. Gular pouch present, well developed in life, indistinct after preservation; distinct transverse gular fold present, deep. Ventral body and limb scales distinctively keeled, more pronounced than those of ventral head, homogeneous in size and shape, mostly regularly arranged.

Coloration. The background coloration of the dorsal and lateral surfaces of the head is pale Light Flesh Color [Color 250] to pale Pink [Color 242]. Three Sepia [Color 286] to Jet Black [Color 300] transverse ornamentation patterns are present on the dorsal surface of the head: the first one is somewhat irregular shaped between the anterior edge of the orbit, the second one is a cross-band between the midpoint of the orbits, and the third one is a X-shaped pattern between the posterior edge of the orbit. All three of these transverse ornamentation patterns extend laterally and enter the orbit on each side of the head; and together with five additional Jet Black [Color 300] streaks or series of speckles on the lateral surface of the head on each side, they form the radial stripe pattern around the eyes. The color of the upper lips and the superior portion of the corner of the mouth are more saturated. Random Sepia [Color 286] to Jet Black [Color 300] short strokes and speckles are also present on the dorsal and lateral surfaces of the head.

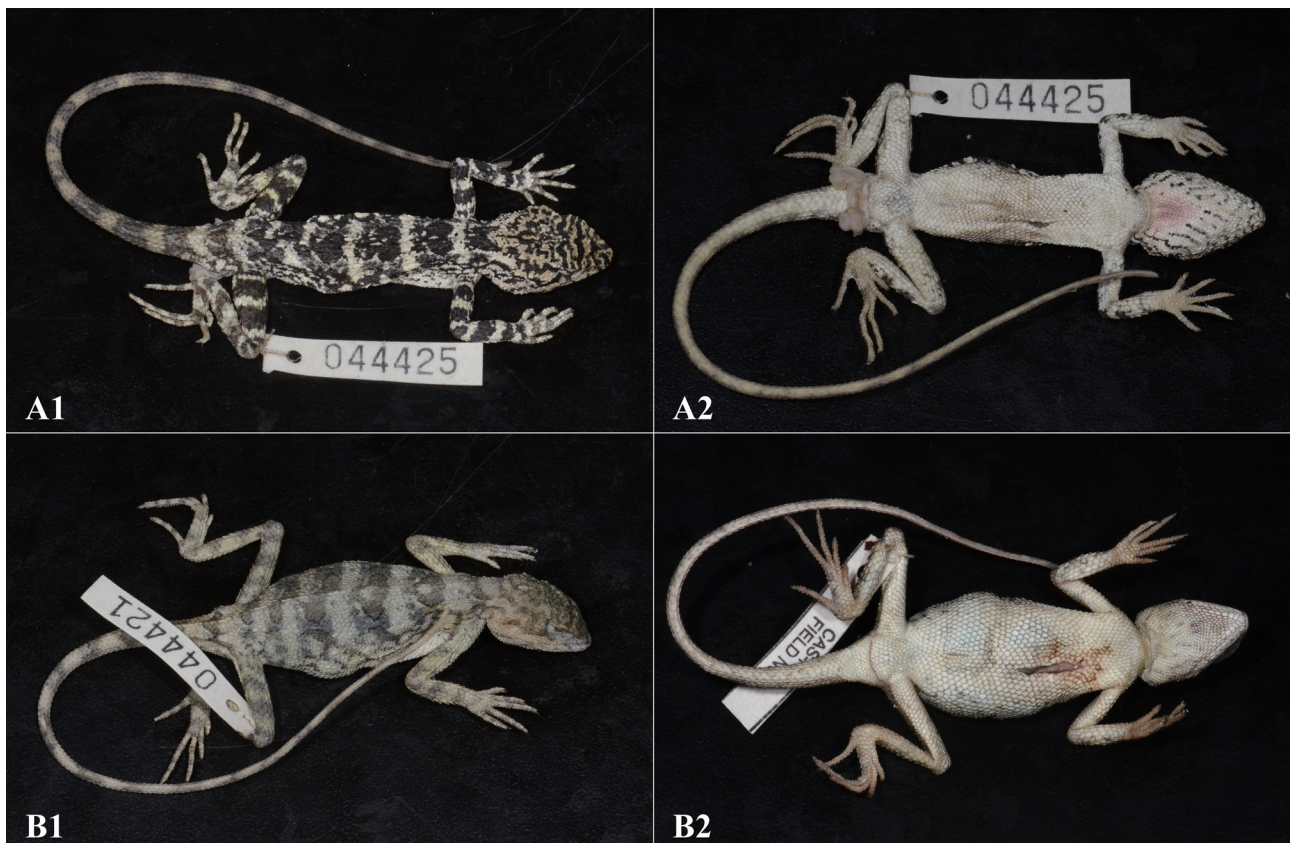


FIGURE 10. Dorsolateral (1) and ventral (2) views of the male holotype KIZ 044425 (A) and female paratype KIZ 044375 (B) of *Diploderma formosgulae* sp. nov. in preservation. Photos by Kai Wang.

The background coloration of the dorsum is Light Buff [Color 2] to Pale Pinkish Buff [Color 3]. A Sepia [Color 286] to Jet Black [Color 300] reticulated ornamentation pattern is present on the lateral surface of the body, inferior to the dorsolateral stripes. A dorsolateral stripe is present on each side of the vertebral crest on the dorsum, running from the neck to the pelvis. This dorsolateral stripe is strongly jagged, with six rhombus-shaped extensions distrib-

TABLE 4. Morphological data of the type series of *D. bowoense* sp. nov. and *D. formosugulae* sp. nov. All morphometric measurements are in the unit of mm, and all paired pholidosis characters are recorded from both sides of the body and are given in left/right order. For measurement methods and abbreviations, see the Methods section. “—” indicates missing data due to an incomplete tail.

Species	<i>D. bowoense</i> sp. nov.			
	Voucher number	KIZ 044700	KIZ 044701	KIZ 044703
Type status	holotype	paratype	paratype	paratype
Sex	M	M	F	F
SVL	53.7	45.7	52.6	54.2
TAL	108.5	86.5	93.2	96.8
HL	15.9	14.1	14.6	15.8
HW	10.3	9.6	10.3	10.5
HD	7.83	7.17	7.82	7.95
SEL	6.28	5.36	6.24	6.78
FLL	24.3	20.8	23.4	24.8
HLL	40.6	33.2	39.2	42.6
T4L	9.7	8.3	9.8	10.2
TRL	24.4	20.4	29.1	29.2
TAL/SVL	201.9%	189.1%	177.3%	178.7%
SEL/HL	39.5%	37.9%	42.7%	43.0%
HW/HL	65.1%	67.8%	70.5%	66.6%
HD/HW	75.7%	74.8%	75.8%	75.8%
FLL/SVL	45.2%	45.4%	44.4%	45.7%
HLL/SVL	75.6%	72.6%	74.6%	78.6%
TRL/SVL	45.3%	44.5%	55.3%	53.9%
SL	10/10	9/8	8/9	8/8
IL	10/12	10/11	10/11	9/10
NSL	2/2	2/1	2/2	2/2
MD	44	42	40	40
F4S	17/16	15/16	15/15	15/14
T4S	21/21	21/18	21/19	19/20
SOR	3/3	4/4	4/4	3/3
PTS	3/3	4/4	4/4	3/4
PTY	5/7	3/4	4/5	4/3
PRS	3/3	4/5	5/6	4/5

TABLE 4. (Continued)

Species		<i>D. formosugulae</i> sp. nov.									
Voucher number	KIZ 044425	KIZ 044417	KIZ 044373	KIZ 044418	KIZ 044420	KIZ 044375	KIZ 044421	KIZ 044423			
Type status	holotype	paratype	paratype	paratype	paratype	paratype	paratype	paratype	paratype	paratype	
Sex	M	M	M	M subadult	F	F	F	F	F	F	
SVL	60.9	57.7	55.5	47.3	60.2	58.6	59.6	55.9			
TAL	119.2	–	–	105.8	113.5	109.0	111.9	108.8			
HL	17.6	17.3	17.3	14.6	17.4	16.5	16.4	15.1			
HW	12.7	11.9	11.6	10.2	12.1	11.2	10.9	11.4			
HD	9.2	8.6	8.5	7.3	8.8	7.8	7.8	7.6			
SEL	6.8	7.0	7.0	5.7	7.0	6.8	6.9	6.2			
FLL	27.3	28.0	27.3	22.0	29.6	28.5	27.8	26.9			
HLL	44.4	44.7	42.9	38.0	46.1	43.0	43.6	42.5			
T4L	9.8	10.6	10.1	9.2	10.6	10.1	9.5	10.0			
TRL	30.2	27.8	27.0	19.8	31.2	32.6	30.3	29.2			
TAL/SVL	195.8%	–	–	223.5%	188.4%	186.1%	187.7%	194.8%			
SEL/HL	38.7%	40.4%	40.3%	39.0%	40.1%	41.3%	42.0%	40.9%			
HW/HL	72.1%	69.1%	66.7%	69.5%	69.4%	68.1%	66.2%	75.4%			
HD/HW	72.6%	71.7%	73.4%	72.0%	72.5%	69.3%	71.8%	66.9%			
FLL/SVL	44.8%	48.6%	49.2%	46.4%	49.1%	48.6%	46.6%	48.2%			
HLL/SVL	73.0%	77.5%	77.4%	80.3%	76.6%	73.4%	73.2%	76.0%			
TRL/SVL	49.5%	48.2%	48.6%	41.9%	51.8%	55.6%	50.8%	52.3%			
SL	10/10	9/9	9/10	10/10	9/9	9/10	9/10	10/10			
IL	11/11	10/10	10/11	12/11	11/11	10/11	10/10	11/11			
NSL	1/1	1/1	2/2	1/1	1/2	1/1	2/2	1/1			
MD	43	39	40	37	40	37	48	42			
F4S	14/14	14/13	16/15	14/14	15/13	14/15	15/15	15/16			
T4S	18/19	19/20	18/19	19/20	21/21	–/20	20/19	23/24			
SOR	3/3	3/3	3/4	3/3	3/3	3/3	3/3	3/3			
PTS	3/3	2/2	3/4	3/5	3/4	3/2	5/4	3/4			
PTY	5/6	4/3	4/4	6/9	8/7	4/6	5/6	5/4			
PRS	4/4	6/7	8/7	8/9	7/6	5/6	4/7	5/6			

uted evenly across the stripe from the shoulder to the pelvis. Such extensions connect dorsally with the counterparts from the other side of the body, forming six transverse streaks across the vertebral crest. The rhombus extensions and their connecting parts of the dorsolateral stripes are Light Buff [Color 2], where the remaining parts of the dorsolateral stripes are muddied with Burnt Umber [Color 48] speckles and patches. The dorsal surfaces of the limbs and tail are Light Buff [Color 2], with evenly distributed Sepia [Color 286] to Jet Black [Color 300] transverse bands or streaks running from the proximal to the distal ends. These streaks get much paler as they approach the distal ends of the fingers, toes, and the tip of the tail.

The ventral surface of the head is white, with Jet Black [Color 300] speckles and short streaks, which is formed by singular rows of black scales. A distinct, triangular shaped gular spot is present at the posterior center of the gular, which is Rose Pink [Color 243] on the peripheral area and Lilac [Color 222] in the center. The ventral surface of the body is uneven Sulphur Yellow [Color 80], which is more saturated towards the anterior portion of each individual scale and paler towards the posterior tip. No other ornamentation is present on the ventral surface of the body. The ventral surfaces of the limbs and the tail are uniform white, except the distal portion, which becomes more brownish.

Variation. Detailed morphological variation is summarized in Table 4. Sexual dimorphism is evident despite the small sample size, in which the males possess relatively longer tail, relatively shorter trunk, and taller nuchal crests (Table 4). Furthermore, similar to most *Diploderma* congeners, *D. formosgulae* **sp. nov.** are sexually dichromatic, where males have different gular coloration than females: for females, the gular spots are less concentrated, and the color is Sulphur Yellow [Color 80]. Among the males, the coloration of gular spot varies from Pinkish Flesh Color [Color 252] in juveniles and subadults (i.e. KIZ 44418, 44424, and 44435) to Rose Pink [Color 243] and Lilac [Color 222] in adults (i.e. KIZ 44425 and 44417).



FIGURE 11. Habitats at the type localities of (A) *Diploderma bowoense* **sp. nov.** and (B) *D. formosgulae* **sp. nov.**; and the observed habitat destructions near the type locality of *D. formosgulae* **sp. nov.** (C1 and C2). Photos by Kai Wang and Wenjie Dong.

Natural history and conservation. *Diploderma formosgulae* **sp. nov.** inhabits the hot-dry valley along the upper Jinsha River in Deqin County, Yunnan Province, China. Individuals were active during the day, basking on rocks and open ground, but slept on low bushes (*Rumex hastatus*) at night. Currently, it is known only along a short section of the upper Jinsha River valley, with an estimated range of about 50km in linear distance, and about 350 km² in area of occupancy. Serious habitat degradation was observed at the type locality, due to both natural causes (i.e. recent flooding from the barrier lake upstream in 2018), as well as anthropogenic causes (i.e. constructions for road repair) (Fig. 11 C1 and C2). In comparison with congeners in the lower reaches of the Jinsha River (i.e. *D. aorun*, and *D. qilin*), the population density of *D. formosgulae* **sp. nov.** is relatively lower. Currently, the new species' range overlaps with major roads and townships in the area, and the habitat is not protected by any existing nature reserve. Following the IUCN listing criteria B 2b (iii) (area of occupancy estimated less than 500km², observed continuing decline in quality of habitat), we recommend listing the new species as Endangered (EN), and we recommend listing it as Class II protected for Chinese Wildlife Protecting Act, in the hope this will bring protection to its degrading valley habitats.

Discussion

Coloration, particularly oral and gular coloration, has been suggested to play an important role in the evolution of *Diploderma* and serves as an important diagnostic character within the genus (Wang *et al.* 2016, 2017, 2019c, 2020b; Fig. 3). In many cases, coloration is the most reliable and diagnostic character that differentiates sister species, as demonstrated in the present study and past literature (Wang *et al.* 2016, 2019c, 2020b). While the oral and gular colorations in *Diploderma* do not go through seasonal changes (shown by captive individuals and field surveys, unpublished data), these colorations do fade or change drastically after long-term preservation. Therefore, documenting coloration in life before preservation is crucial in the modern taxonomy of the genus *Diploderma*. However, to date, several species continue to lack information about their coloration in life, including *D. grahami* and *D. hamptoni*. Both of these species are known only from descriptions of the holotype specimens, each more than 100 years old, and no live individuals have been documented since their original descriptions. Further taxonomic studies should focus on these taxa to increase our understanding of their ecology and natural history, current distribution, and phenotypic variation, including coloration in life. For the purpose of diagnosing and cataloguing existing historical museum specimens, as most *Diploderma* species, particularly those that are similar in morphometric and pholidosis characters, are microendemic in isolated river valleys, locality information can aid the taxonomic identifications greatly when such information is available. Unfortunately, if historical collections do not have precise locality information and the diagnostic morphological characters lead to similar species that are only diagnostic by live coloration, identification of specimens could be challenging, and ancient DNA extraction and barcoding method may be the best way for proper species identification in these cases.

While considerable progress has been made on the taxonomy of *D. flaviceps* complex in Southwest China, particular along the upper Jinsha (Wang *et al.* 2020b) and upper Mekong River (Wang *et al.* 2016, 2019b), much needs to be done regarding the remaining river valleys in the HMR, particularly the upper Salween River in Tibet. Our present study and past studies (Wang *et al.* 2019b, 2020b) have demonstrated the “predictable” pattern of distribution of *Diploderma* in the northern HMR, and the current pattern indicates a high possibility of having overlooked diversity in the large gap regions in the upper Salween River (Fig. 1). Future studies should focus on these regions and assess the taxonomic status of the resulting *Diploderma* populations.

Recent studies have stressed the urgent conservation needs of neglected valley ecosystems in the HMR, both for the endemic flora (Zhang *et al.* in press) and for the microendemic *Diploderma* diversity specifically (Wang *et al.* 2016, 2017, 2019b, 2020b). Our discoveries of the two micro-endemic new species here further highlight the importance of the previously neglected hot-dry valley habitats to endemic vertebrate biodiversity in the HMR. We recommend extending the existing nature reserves in the HMR to cover the unique hot-dry valley habitats and establishing additional micro-reserves in the non-protected valleys.

Lastly, despite the gradual clarification of *Diploderma* taxonomy, very little is known about the general biology of the genus, particularly fine-scale distribution data, population trends, diet and ecological interactions, behavior characteristics, and evolutionary studies. We recommend future studies take advantage of the revised taxonomy and explore the different aspects of biology of these unique agamid species in the HMR.

Acknowledgements

Collection permits were issued by Kunming Institute of Zoology, Chinese Academy of Sciences (BBCJ-2014-001). We followed IACUC protocols (IACUC R13-11) and relevant protocols of the Animal Care and Ethics Committee at the Kunming Institute of Zoology, Chinese Academy of Sciences for the proper treatments of animals in the field. We thank Mr. Ciren Zhongyang, Mr. Xiankun Huang, Mr. Man Fu, and Mr. Zhuoyu Lu for their assistance in the field; Dr. V. Deepak for his helps in examining specimens at NHM and taking photographs; Dr. Jiatang Li (CIB), Mr. Ke Jiang (CIB), Mr. Jinlong Ren (CIB), Drs. Rafe Brown and Luke Welton (KU), Mr. Wynn Addison (NMNH), Mr. Jens Vindum and Ms. Lauren Scheinberg (CAS), and Drs. James Hanken and Jonathan Losos (MCZ) for their supports in allowing us examine specimens or facilitate specimen loans; and Mr. Zhongbing Yu for taking photos of voucher specimens. This research was supported by the Second Tibetan Plateau Scientific Expedition and Research (STEP) program (2019QZKK0501), the Strategic Priority Research Program of Chinese Academy of Sciences (XDA20050201), the National Key Research and Development Program of China (2017YFC0505202), China's Biodiversity Observation Network (Sino-BON), and the Animal Branch of the Germplasm Bank of Wild Species, CAS (Large Research Infrastructure Funding) to CJ; NSF DEB 1657648 to CDS; NSF GRFP 2017216966 and EAPSI 1714006 to KW; and the Biodiversity Survey and Assessment Project of the Ministry of Ecology and Environment (2019HJ2096001006) to JJ and QY.

References

- Barbour, T. & Dunn, E.R. (1919) Two new Chinese Japaluras. *Proceedings of the New England and Zoological Club*, 7, 15–19.
- Denzer, W., Manthey, U. & Campbell, P.D. (2019) Catalogue of type specimens of the agamid lizard genus *Japalura* s. l. (Squamata: Agamidae: Draconinae) *Zootaxa*, 4612 (1), 109–125.
<https://doi.org/10.11646/zootaxa.4612.1.8>
- Dong, F., Hung, C. & Yang X. (2020) Secondary contact after allopatric divergence explains avian speciation and high species diversity in the Himalayan-Hengduan Mountains. *Molecular Ecology and Evolution*, 143, 106671.
<https://doi.org/10.1016/j.ympev.2019.106671>
- Hu, S., Zhao, E., Jiang, Y., Fei, L., Ye, C., Hu, Q., Huang, Q., Huang, Y. & Tian, W. (1987) *Amphibia-Reptilia of Xizang*. Science Press, Beijing, 153 pp. [in Chinese]
- Köhler, G. (2012) *Color Catalogue for Field Biologists*. Herpeton, Offenbach, Hesse, 49 pp.
- Liu, S., Hou, M., Wang, J., Ananjeva, N.B. & Rao, D. (2020) A new species of *Diploderma* (Squamata: Sauria: Agamidae) from Yunnan Province, China. *Russian Journal of Herpetology*, 27, 127–148.
<http://dx.doi.org/10.30906/1026-2296-2020-27-3-127-148>.
- Manthey, U., Wolfgang, D., Hou, M. & Wang, X. (2012) Discovered in historical collections: two new *Japalura* species Squamata: Sauria: Agamidae from Yulong Snow Mountains, Lijiang Prefecture, Yunnan, PR China. *Zootaxa*, 3200 (1), 27–48.
<http://dx.doi.org/10.11646/zootaxa.3200.1.2>
- Ronquist, F., Teslenko, M., Van Der Mark, P., Ayres, D.L., Darling, A., Höhna, S., Larget, B., Liu, L., Suchard, M.A. & Huelsenbeck, J.P. (2012) MrBayes 3.2: efficient Bayesian phylogenetic inference & model choice across a large model space. *Systematic Biology*, 61, 539–542.
<http://doi.org/10.1093/sysbio/sys029>
- Smith, M.A. (1935) *The Fauna of British India, including Ceylon and Burma. Reptiles and Amphibia, Vol. II. Sauria*. Taylor and Francis, London, 440 pp.
- Stamatakis, A. (2014) RAxML version 8: a tool for phylogenetic analysis & post analysis of large phylogenies. *Bioinformatics*, 30, 1312–1313.
<https://doi.org/10.1093/bioinformatics/btu033>
- Stejneger, L.H. (1924) Herpetological novelties from China. *Occasional Papers of the Boston Society of Natural History*, 5, 119–121.
- Stuart-Fox, D.M. & Ord, T.J. (2004) Sexual selection, natural selection and the evolution of dimorphic coloration and ornamentation in agamid lizards. *Proceedings of the Royal Society B*, 271, 2249–2255.
<https://doi.org/10.1098/rspb.2004.2802>
- Swofford, D.L. (2002) *PAUP*4.0. Phylogenetic Analysis Using Parsimony, Version 4.0b10*. Sinauer Associates, Sunderland, Massachusetts.
- Wang, K., Jiang, K., Pan, G., Hou, M., Siler, C.D. & Che, J. (2015) A new species of *Japalura* Squamata: Sauria: Agamidae from Eastern Tibet, PR China. *Asian Herpetological Research*, 6, 159–168.
<http://doi.org/10.16373/j.cnki.ahr.140042>
- Wang, K., Jiang, K., Zou, D., Yan, F., Siler, C.D. & Che, J. (2016) Two new species of *Japalura* (Squamata: Sauria: Agamidae)

- from the Hengduan Mountain Range, PR China. *Zoological Research*, 37, 41–56.
<https://doi.org/10.13918/j.issn.2095-8137.2016.1.41>
- Wang, K., Ren, J., Jiang, K., Yuan, Z., Che, J. & Siler, C.D. (2017) Rediscovery of the enigmatic mountain dragon, *Japalura yulongensis* Reptilia: Sauria: Agamidae, with notes on its natural history and conservation. *Zootaxa*, 4318 (2), 351–363.
<http://doi.org/10.11646/zootaxa.4318.2.8>
- Wang, K., Che, J., Lin, S., Deepak, V., Aniruddha, D., Jiang, K., Jin, J., Chen, H. & Siler, C.D. (2019a) Multi-locus phylogeny & taxonomic revision of the Mountain Dragons of the genus *Japalura* s. l. Gray, 1853 “Reptilia: Squamata: Agamidae”. *Zoological Journal of the Linnean Society*, 185, 246–267.
<https://doi.org/10.1093/zoolinnean/zly034>
- Wang, K., Jiang, K., Ren, J., Zou, D., Wu, J., Che, J. & Siler, C.D. (2019b) A new species of dwarf *Japalura* Reptilia: Squamata: Agamidae from the upper Mekong River in Eastern Tibet, with notes on morphological variation, distribution, & conservation of two congeners along the same river. *Zootaxa*, 4544 (4), 505–522.
<https://doi.org/10.11646/zootaxa.4544.4.3>
- Wang, K., Wu, J., Jiang, K., Chen, J., Miao, B., Siler, C.D. & Che, J. (2019c) A new species of mountain dragon Reptilia: Agamidae: *Diploderma* from the *D. dymondi* complex in southern Sichuan Province, China. *Zoological Research*, 40, 456–465.
<https://doi.org/10.24272/j.issn.2095-8137.2019.034>
- Wang, K., Ren, J., Jiang, K., Wu, J., Yang, C., Xu, H., Messenger, K., Lei, K., Yu, H., Yang, J., Siler, C.D., Li, J. & Che, J. (2019d) Revised distribution of some species in the genus *Diploderma* (Reptilia: Agamidae) in China. *Sichuan Journal of Zoology*, 38, 481–495. [in Chinese]
<http://doi.org/10.11984/j.issn.1000-7083.20180405>
- Wang, K., Ren, J., Chen, H., Lyu, Z., Guo, X., Chen, J., Jiang, K., Li, J., Guo, P., Wang, Y. & Che, J. (2020a) The updated checklists of amphibians and reptiles of China. *Biodiversity Science*, 28, 189–218.
<https://doi.org/10.17520/biods.2019238>
- Wang, K., Ren, J., Wu, J., Jiang, K., Jin, J., Hou, S., Zheng, P., Xie, F., Siler, C.D. & Che, J. (2020b “2021”) Systematic revision of Mountain Dragons (Reptilia: Agamidae: *Diploderma*) in China, with descriptions of six new species and discussion on their conservation. *Journal of Zoological Systematics and Evolution*, 59, 222–263.
<https://doi.org/10.1111/jzs.12414>
- Yang, D. & Rao, D. (2008) *Amphibia and Reptilia of Yunnan*. Yunnan Science and Technology Press, Kunming, Yunnan, 411 pp. [in Chinese]
- Zhang, Y., Qian, L., Spalink, D., Sun, L., Chen, J. & Sun, H. (2021) Spatial phylogenetics of two topographic extremes of the Hengduan Mountains in southwestern China and its implications for biodiversity conservation. *Plant Diversity*, in press.
<https://doi.org/10.1016/j.pld.2020.09.001>
- Zhao, E. & Yang, D. (1997) *Amphibians and Reptiles of the Hengduan Mountain Region*. Science Press, Beijing, 303 pp. [in Chinese]
- Zhao, E., Zhao, K. & Zhou, K. (1999) *Fauna Sinica, Reptilia, Vol. 2: Squamata, Lacertilia*. Science Press, Beijing, 394 pp. [in Chinese]
- Zhao, E. (2003) *Colored Atlas of Reptiles of Sichuan*. China Forestry Publishing House, Chengdu, Sichuan, 292 pp. [in Chinese]

APPENDIX I. Specimens of recognized species of the genus *Diploderma* examined in this study. Museum abbreviations include the following: Museum of Kunming Institute of Zoology, Chinese Academy of Sciences (KIZ); Museum of California Academy of Sciences (CAS), San Francisco, CA, USA; Chengdu Institute of Biology, Chinese Academy of Sciences (CIB); Kunming Institute of Zoology, Chinese Academy of Sciences (KIZ), Kunming, Yunnan, China; University of Kansas Biodiversity Institute (KU), Lawrence, KS, USA; Field Museum of Natural History (FMNH), Chicago, IL, USA; Museum of Comparative Zoology (MCZ), Cambridge, MA, USA; Natural History Museum (NHM), London, UK; and Smithsonian National Museum of Natural History (USNM).

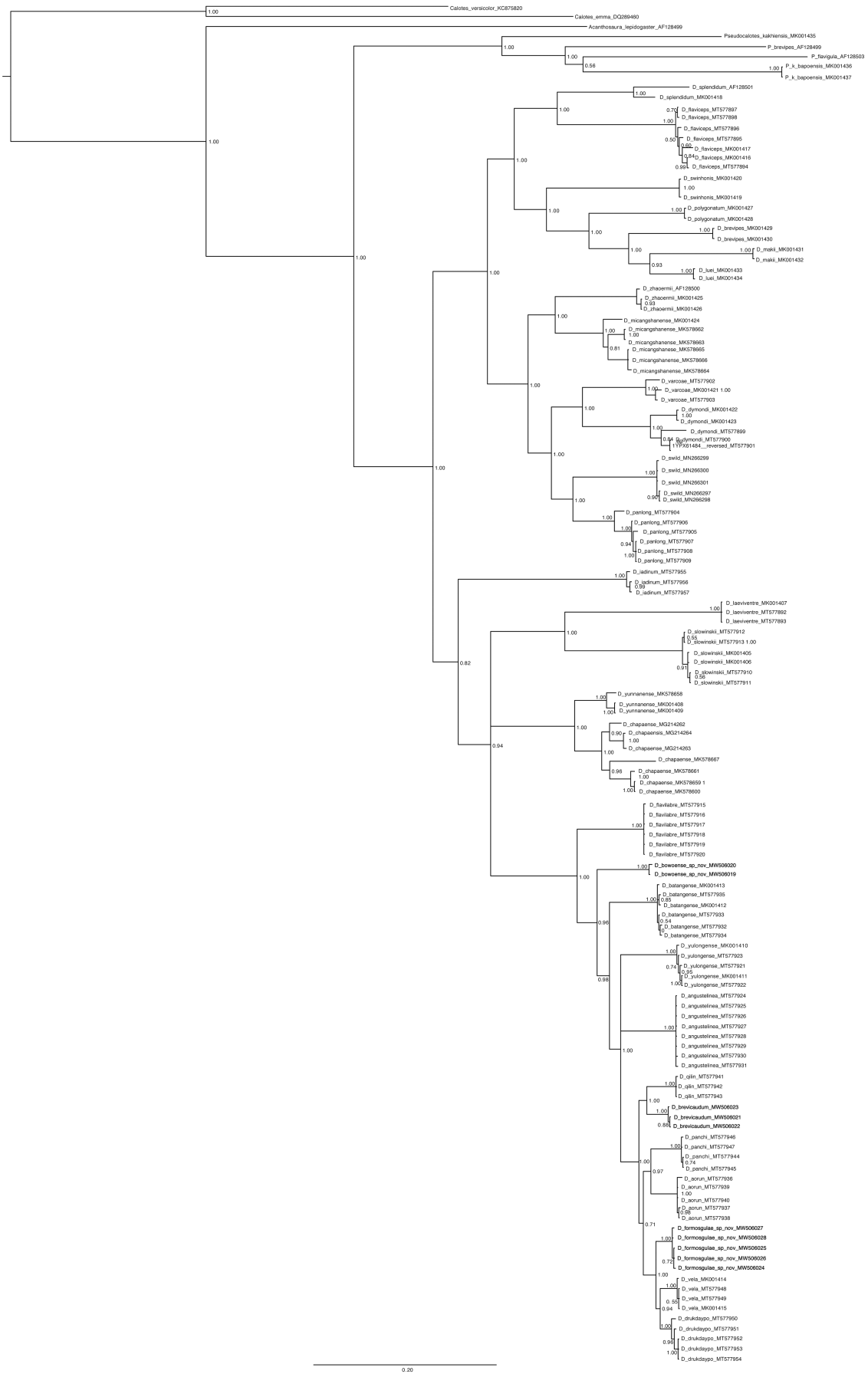
- D. angustelinea* (n=10): KIZ 029703 (holotype), KIZ 044484, 044796, 044797, 029404–029408, 029710 (paratypes), Maidilong Village, Muli, Sichuan, China.
- D. aorun* (n=13): KIZ 044735 (holotype), Dari Village, Deqin, Yunnan, China; KIZ 032734, 032736, 032737, 032735, near Benzilan township, Deqin, Yunnan Province, China; KIZ 044431, 044432, 044433, Rongzong Village, Deqin, Yunnan, China; KIZ 044740, 044742, near Zhidu, Deqin, Yunnan, China; CIB 116315–16, CIB 116318, from Songmai Township, Derong, Sichuan China; KIZ 044764, near Derong township, Sichuan, China (all paratypes).
- D. batangense* (n=18): KIZ 019276–019279, 019281, 019282, 019285, 019286, 044729, 044731, 044765, 044766, 044769, 044783, 044787 (topotypes), Batang, Sichuan, China; KIZ 09404, 019312, 019314, Mangkang, Tibet, China.
- D. chapaense* (n=6): CIB 2679/583623, KIZ 047085, Jingdong, Yunnan Province, China. KIZ 040145, Dali, Yunnan, China; KIZ 034921–23, Lvchun, Yunnan, China.
- D. drukdaypo* (n=8): KIZ 027616 (holotype), KIZ 027618, 027619, 027628–027630 (paratypes), Chaya, Chamdo, Tibet, China; KIZ 016486 (paratype), Karuo, Chamdo, Tibet, China.
- D. dymondi* (n=20): KIZ 040639, 040640 (topotypes), Dongchuan, Yunnan, China; KIZ 040147–040153, CIB 1869/755156, City of Panzhihua, Panzhihua District, Sichuan, China; KIZ 9511001, 9511002, 9511016, 9511018, 9511022, KIZ 040645–48, Dayao, Yunnan, China; CIB 1870/65I5020, Yuzha, Huili County, Liangshan Prefecture, Sichuan, China.
- D. fasciatum* (n=3): CIB 2620–2622, Peng County, Sichuan, China.
- D. flaviceps* (n=15): CIB 2234, 2332, 2333, 2341, 2354, 2355, 2549, 2554, 2556, 2561, 2567; KIZ 05181, 05182, 84001 (topotypes), Luding, Sichuan, China; KU 208076 (topotype), Luding, Sichuan, China.
- D. flavilabre* (n=8): KIZ 032693 (holotype), 032692, 032694, 032695–032699, 032730 (paratypes), Yebatan, Gaiyu, Sichuan, China.
- D. grahami* (n=1): USMN 65500 (holotype), Yibin, Sichuan, China.
- D. hamptoni* (n=1): BMNH 1908.9.18.1/1946.8.14.1 (holotype), Mogok, Myanmar.
- D. iadinum* (n=16): KIZ 019321 (holotype), 09398 (allotype), 09401–03, 019322, 019325–019328 (paratypes), Ninong, Deqin, Yunnan, China; KIZ 027702–05, Yunling, Deqin, Yunnan, China.
- D. laeviventre* (n=5): KIZ 014038 (holotype), 014037, 014041–014043 (paratypes), Markam, Tibet, China.
- D. makii* (n=2): MCZ R-172743 (paratype), R-181443, Nantong, Taiwan, China.
- D. micangshanense* (n=9): CIB 86348, 86351, Xianyang, Shaanxi, China; CIB 86356, 86357, 86360, 86361, Luonan, Shaanxi, China; CIB 2572, 2578, 2582, Wenxian, Gansu, China.
- D. panchi* (n=4): KIZ 032715 (holotype), 032716, 032717, 032729 (paratypes), Yajiang Township, Ganzi, north-west Sichuan Province, China.
- D. panlong* (n=7): KIZ 040138 (holotype), 040137, 040139, 040140, 040143, 040141, 040142 (paratypes), Miansha Village, Mianning, Sichuan, China.
- D. polygonatum* (n=11): MCZ 45954, 45956 (paratypes), CAS 21215, 21355, 21243, 21221, 21244, Okinawa, Japan.
- D. qilin* (n=13): KIZ 028332 (holotype); paratypes: 028333, 028334–336, Balong, Deqin County, Yunnan, China; KIZ 044412, 044413, Baka Village, Shangri-La, Yunnan, China; KIZ 044405, 044407, 044408, Meiding Village, Shangri-La, Yunnan, China; KIZ 044745, 044744, Cangjue Village, Shangri-La, Yunnan, China; KIZ 044820, Pengnanshou Bridge, Shangri-La, Yunnan, China.
- D. splendidum* (n=6): USNM 35522 (holotype), Yichang, Hubei, China; CIB 2588, 2591, 2596, 72468, 72469, Chongqing, China.

- D. slowinskii* ($n=11$): KIZ 027541, 027543, 027572–74, 027577, 027579, 027595, 027596, 027598, 027600 (topotypes), Nujiang Prefecture, Yunnan, China.
- D. swild* ($n=8$): KIZ 034912 (holotype), 034894, 034913, 034914, 040125–27 (paratypes), Panzihua, Sichuan, China; CIB 1871/105074 (paratype), Xichang, Liangshan Prefecture, Sichuan, China.
- D. swinhonis* ($n=4$): CAS 18085, 18089, 18098, 18099, Taiwan, China.
- D. varcoae* ($n=15$): KIZ 85I0006, 85I0009, 83001, 034294 (topotypes), Kunming, Yunnan, China; KIZ 015691, Yuxi, Yunnan, China; KIZ 015689, Mengzi, Honghe Prefecture, Yunnan, China; CIB 2682/625219, 2659/625233, 2657/625212, 2660/625213, 2668/625214, 2667/625215, 2666/625217, 2662/625218, 2658/625221, 2679/583623, Jizu Mountain, Dali, Yunnan Province.
- D. vela* ($n=31$): KIZ 013801 (holotype), KIZ 013802, 013813, 013800, 013805–013811 (paratypes), Jerkalo, Tibet, China; KIZ 027641, 027645–49, Rumei, Markam, Tibet, China; KIZ 027668, 027670–73, Tongsha, Markam, Tibet, China; KIZ 027667, 027693–695, Foshan, Deqin, Yunnan, China; KIZ 027680, 027681, Xilu, Deqin, Yunnan, China; KIZ 027682, 027684, Xidang, Deqin, Yunnan, China.
- D. yulongense* ($n=15$): KIZ 09399, 09400, 028291–028293, 028294, 028296–028298, 028299, 028300, 028303, 028342–028344, Xianggelila County, Yunnan, China.
- D. yunnanense* ($n=8$): CIB 2684, 2686, 2687, 2689, KIZ 82081 (topotypes), Longling, Yunnan, China; KIZ 74II0240, 0248, 79I469, Tengchong, Yunnan, China; KIZ 040193, Yingjiang, Yunnan, China.
- D. zhaoermii* ($n=14$): CIB 2690 (holotype), 86432, 86435, 85721, 85722, 86433, 86434, 86436, Wenchuan, Sichuan, China; CIB 2232, 2244, 2240, KIZ 84032, 85030, Lixian, Sichuan, China.

SUPPLEMENTARY TREE FILES. Each sequence is denoted by “genus_species” name and ended with its corresponding GenBank accession number.



S1. RAxML topology



S2. Bayesian topology